



Supporting Information

The Six Isomers of the Cyclohexanol Dimer: A Delicate Test for Dispersion Models

*Marcos Juanes, Imanol Usabiaga, Iker León, Luca Evangelisti, José A. Fernández, and Alberto Lesarri**

ange_202005063_sm_miscellaneous_information.pdf

CONTENTS

Experimental and theoretical methods

Figures

Figure S1. Microwave spectrum of cyclohexanol in the region 2-8 GHz, with x 10 and x 20 expansions of the vertical axis (10^6 averages).

Figure S2. Horizontal expansions of the microwave spectrum of cyclohexanol (x 20).

Figure S3. Isomer I (=AT(2)EG-) structure according to B3LYP-D3(BJ)/def2TZVP DFT calculations (rotatable 3D figure in pdf file; atomic coordinates collected in Table S11).

Figure S4. Isomer II (=EG-(2)EG-) structure according to B3LYP-D3(BJ)/def2TZVP DFT calculations (rotatable 3D figure in pdf file; atomic coordinates collected in Table S12).

Figure S5. Isomer III (=EG-(1)AG-) structure according to B3LYP-D3(BJ)/def2TZVP DFT calculations (rotatable 3D figure in pdf file; atomic coordinates collected in Table S13).

Figure S6. Isomer IV (=EG-(1)AG+) structure according to B3LYP-D3(BJ)/def2TZVP DFT calculations (rotatable 3D figure in pdf file; atomic coordinates collected in Table S14).

Figure S7. Isomer V (=AG-(1)EG+) structure according to B3LYP-D3(BJ)/def2TZVP DFT calculations (rotatable 3D figure in pdf file; atomic coordinates collected in Table S15).

Figure S8. Isomer VI (=EG-(1)EG+) structure according to B3LYP-D3(BJ)/def2TZVP DFT calculations (rotatable 3D figure in pdf file; atomic coordinates collected in Table S16).

Figure S9. Relative stability of the cyclohexanol monomer as a function of temperature (M06-2X/6-311++G(d,p))

Figure S10. Equatorial-to-axial estimated interconversion barriers for the cyclohexanol monomer starting from an equatorial gauche (EG) geometry and using six different interconversion paths. The reaction barriers are estimations, since no transition-state calculation has been performed. The calculated conformational stabilities gave barrier heights of 47-51 kJ mol⁻¹ using M06-2X/6-311++G(d,p). Similar barriers of 49-54 kJ mol⁻¹ are obtained when starting from an equatorial trans (ET) geometry (not shown).

Figure S11. Equatorial-to-axial estimated interconversion barriers for the cyclohexanol dimer starting from the six observed dimer geometries. The reaction barriers are estimations, since no transition-state calculation has been performed. Each

interconversion barrier is the average over six interconversion paths using as inversion coordinate the dihedrals C1-C2-C3-C4, C2-C3-C4-C5, C3-C4-C5-C6, C4-C5-C6-C1, C5-C6-C1-C2 and C6-C1-C2-C3. The conformational stabilities were calculated with M06-2X/6-311++G(d,p) and gave barriers heights of 44-51 kJ mol⁻¹.

Figure S12. Reduced electronic density gradient s ($= \frac{1}{2(3\pi^2)^{1/3}} \frac{|\nabla\rho|}{\rho^{4/3}}$) vs. the signed electronic density ($= \text{sign}(\lambda_2)\rho$) and NCIPlot for isomer I (=AT(2)EG-) of the cyclohexanol dimer. The plot minimum at negative coordinates indicates a bond critical point and the presence of a O-H···O hydrogen bond interaction. Minima close to the origin denote weak interactions, while the positive minimum is indicative of repulsive interactions like ring critical points. The color scale of the molecular drawing corresponds to attractive interactions (blue), weak interactions (green) or repulsive interactions (red).

Figure S13. Reduced electronic density gradient s ($= \frac{1}{2(3\pi^2)^{1/3}} \frac{|\nabla\rho|}{\rho^{4/3}}$) vs. the signed electronic density ($= \text{sign}(\lambda_2)\rho$) and NCIPlot drawing for isomer II (=EG-(2)EG-) of the cyclohexanol dimer.

Figure S14. Reduced electronic density gradient s ($= \frac{1}{2(3\pi^2)^{1/3}} \frac{|\nabla\rho|}{\rho^{4/3}}$) vs. the signed electronic density ($= \text{sign}(\lambda_2)\rho$) and NCIPlot drawing for isomer III (=EG-(1)AG-) of the cyclohexanol dimer.

Figure S15. Reduced electronic density gradient s ($= \frac{1}{2(3\pi^2)^{1/3}} \frac{|\nabla\rho|}{\rho^{4/3}}$) vs. the signed electronic density ($= \text{sign}(\lambda_2)\rho$) and NCIPlot drawing for isomer IV (=EG-(1)AG+) of the cyclohexanol dimer.

Figure S16. Reduced electronic density gradient s ($= \frac{1}{2(3\pi^2)^{1/3}} \frac{|\nabla\rho|}{\rho^{4/3}}$) vs. the signed electronic density ($= \text{sign}(\lambda_2)\rho$) and NCIPlot drawing for isomer V (=AG-(1)EG+) of the cyclohexanol dimer.

Figure S17. Reduced electronic density gradient s ($= \frac{1}{2(3\pi^2)^{1/3}} \frac{|\nabla\rho|}{\rho^{4/3}}$) vs. the signed electronic density ($= \text{sign}(\lambda_2)\rho$) and NCIPlot drawing for isomer VI (=EG-(1)EG+) of the cyclohexanol dimer.

Tables

Table S1. Measured rotational transitions of the isomer I (= AT(2)EG-) of the cyclohexanol dimer, residuals according to fit of Table 1 and assumed experimental uncertainties (all values in MHz).

Table S2. Measured rotational transitions of the isomer II (= EG-(2)EG-) of the cyclohexanol dimer, residuals according to fit of Table 1 and assumed experimental uncertainties (all values in MHz).

Table S3. Measured rotational transitions of the isomer III (= EG-(1)AG-) of the cyclohexanol dimer, residuals according to fit of Table 1 and assumed experimental uncertainties (all values in MHz).

Table S4. Measured rotational transitions of the isomer IV (= EG-(1)AG+) of the cyclohexanol dimer, residuals according to fit of Table 1 and assumed experimental uncertainties (all values in MHz).

Table S5. Measured rotational transitions of the isomer V (= AG-(1)EG+) of the cyclohexanol dimer, residuals according to fit of Table 1 and assumed experimental uncertainties (all values in MHz).

Table S6. Measured rotational transitions of the isomer VI (= EG-(1)EG+) of the cyclohexanol dimer, residuals according to fit of Table 1 and assumed experimental uncertainties (all values in MHz).

Table S7. Conformational search of the cyclohexanol dimer using the DFT method B3LYP-D3(BJ)/def2-TZVP. For each isomer the table presents the rotational constants (A , B , C), the relative electronic energy (ΔE , including zero-point and BSSE corrections), the relative Gibbs energy (ΔG , at 1 atm and 298 K) and the relative binding (free) energies (BE) at temperatures of 0 K and 298 K. The binding free energies are calculated as differences between the Gibbs energy in the complex and the sum of the Gibbs energies in the two monomers, with the monomer structures corresponding to the most similar stable conformation compared with the structure adopted in the complex.

Table S8. Conformational search of the cyclohexanol dimer using the DFT method MN15-L/def2-TZVP. For each isomer the table presents the rotational constants (A , B , C), the relative electronic energy (ΔE , including zero-point and BSSE corrections), the relative Gibbs energy (ΔG , at 1 atm and 298 K) and the relative binding (free) energies

(BE) at temperatures of 0 K and 298 K. The binding free energies are calculated as differences between the Gibbs energy in the complex and the sum of the Gibbs energies in the two monomers, with the monomer structures corresponding to the most similar stable conformation compared with the structure adopted in the complex.

Table S9. Conformational search of the cyclohexanol dimer using the DFT method M06-2X-6-311++G(d,p). For each isomer the table presents the rotational constants (A , B , C), the relative electronic energy (ΔE , including zero-point and BSSE corrections), the relative Gibbs energy (ΔG , at 1 atm and 298 K) and the relative binding (free) energies (BE) at temperatures of 0 K and 298 K. The binding free energies are calculated as differences between the Gibbs energy in the complex and the sum of the Gibbs energies in the two monomers, with the monomer structures corresponding to the most similar stable conformation compared with the structure adopted in the complex.

Table S10. Comparison of experimental and predicted rotational parameters for the six observed isomers of the cyclohexanol dimer, using the DFT methods B3LYP-D3(BJ) and ω B97XD (def2-TZVP basis set). The relative differences of the predicted rotational constants with the experimental values are shown in square brackets. The complexation energy (E_c) corresponds to the difference between the electronic energy of the dimer and the sum of the monomers in the dimer configuration, including BSSE corrections (see Table S17 for the SAPT2+(3) binding energy calculation).

Table S11. Atomic coordinates for isomer I (= EG-(1)AG-) of the cyclohexanol dimer according to B3LYP-D3(BJ)/def2TZVP DFT calculations (principal axes system).

Table S12. Atomic coordinates for isomer II (= EG-(1)AG+) of the cyclohexanol dimer according to B3LYP-D3(BJ)/def2TZVP DFT calculations (principal axes system).

Table S13. Atomic coordinates for isomer III (= EG-(2)EG-) of the cyclohexanol dimer according to B3LYP-D3(BJ)/def2TZVP DFT calculations (principal axes system).

Table S14. Atomic coordinates for isomer IV (= AT(2)EG-) of the cyclohexanol dimer according to B3LYP-D3(BJ)/def2TZVP DFT calculations (principal axes system).

Table S15. Atomic coordinates for isomer V (= EG-(1)EG+) of the cyclohexanol dimer according to B3LYP-D3(BJ)/def2TZVP DFT calculations (principal axes system).

Table S16. Atomic coordinates for isomer VI (= EG-(1)EG+) of the cyclohexanol dimer according to B3LYP-D3(BJ)/def2TZVP DFT calculations (principal axes system).

Table S17. Results from a second-order intramonomer / third-order intermonomer Symmetry-Adapted Perturbation Theory (SAPT2+(3)/aug-cc-pVDZ) binding energy decomposition of $(\text{cyclohexanol})_2$ and related dimers, comparing the magnitude of the electrostatic and dispersion contributions, together with available reference values from the S22 database (all values in kJ mol^{-1}).

Experimental and theoretical methods

A sample of cyclohexanol (99%) was obtained commercially and used without further purification. The sample is liquid at room temperature (m.p. 20-24°C, b.p. 160-161°C), so it was heated inside a reservoir nozzle (60-80°C) to ensure sufficient vapor pressure (75 hPa at 94°C). A molecular jet was created by co-expanding cyclohexanol with a stream of pure neon (99.999%) at backing pressures of 0.1-0.3 MPa, using a single nozzle with circular orifices of 0.8 or 1.0 mm. In additional experiments helium or argon (99.999%) were used as carrier gases. The gas pulses extended typically for 500-900 μs depending on the carrier gas, and propagated perpendicularly to the emitting and receiving broadband horn antennas. The expansion chamber was evacuated with an oil diffusion pump and a primary rotary pump to ultimate pressures of ca. 10⁻⁷ hPa.

The chirped-pulsed Fourier transform microwave (CP-FTMW) spectrometer uses a direct-digital design following Pate,^[1-3] covering the 2-8 GHz frequency range.^[4] In this experiment, the jet was probed with short (4 μs) chirped-pulses spanning the full 6 GHz bandwidth, using sequences of 5 microwave exciting pulses per molecular gas pulse. Each chirped-pulse was amplified to a nominal power of 20 W and radiated into the jet. Detection of the transient emission resulting from rotational decoherence used a digital oscilloscope (20 MSamples/s) and extended for 40 μs per excitation pulse. The time-domain data were Fourier transformed using a Kaiser-Bessel window,^[5] producing linewidths of ca. 100 kHz. Frequency uncertainties are estimated as 10 kHz. For the present purposes ca. 1 M spectral averages were acquired at a repetition rate of 5 Hz. The relative intensity measurements^[6,7] were conducted on 20 μ_a R-branch ($J'+1 \leftarrow J''$) rotational transitions with quantum numbers $J''=3-8$, $K_{\perp}=0-3$ (2-6 GHz). The derived jet populations are dependent on several theoretical and experimental assumptions, and should be taken as approximations. This calculation assumed a linear fast-passage polarization regime, with signal intensities proportional to the squared dipole moments and population differences ($\Delta N_{12} \mu_{12}^2$).^[3] The instrumental response was considered uniform and the electric dipole moments were taken from the B3LYP-D3(BJ) prediction in Table S10, which makes the results dependent of the computational model. In these conditions, isomer I, predicted with the smallest dipole moment, appears as most populated, while expansion experiments with argon indicate that the global minimum

is one of isomers II, III or IV. This fact is indicative of model deficiencies in the calculation of relative populations.

The experiment was supported by several computational Chemistry methods. The initial survey of the potential energy surface of the cyclohexanol dimer used the molecular mechanics MMFFs force field,^[8] and conformational searching routines implemented in MacroModel.^[9]

Molecular orbital calculations were performed using Kohn-Sham density-functional-theory (DFT).^[10] The selected functionals included the Truhlar's parametrizations for non-covalent interactions MN15-L^[11] and M06-2X^[12] and Becke's hybrid three-parameter B3LYP^[13] method including two-body Grimme D3^[14] dispersion corrections with Becke-Johnson damping.^[15,16] The six final isomers were later reoptimized with the Head-Gordon's hybrid ω B97X-D method.^[17] The basis set chosen for the present calculations was Ahlrichs' balanced polarized triple- ζ def2-TZVP.^[18] DFT calculations were implemented in Gaussian09 and Gaussian16.^[19]

A categorization of the physical forces stabilizing the cyclohexanol dimer was obtained from a symmetry-adapted perturbation theory^[20,21] (SAPT) analysis implemented in PSI4,^[22] producing a binding energy decomposition. This perturbative calculation used second-order intramonomer correlation corrections and up to third-order intermonomer dispersion corrections denoted SAPT2+(3)^[23] and a double- ζ aug-cc-pVDZ basis set. The interaction energy is decomposed into electrostatic (ΔE_{elec}), inductive (multipole interactions/charge transfer, ΔE_{ind}), exchange repulsion (ΔE_{exch}) and dispersion (ΔE_{disp}) energy terms.

The analysis of the non-covalent interactions in the dimer used a 3-D representation of the reduced gradient of the electronic density, as implemented in NCIPlot.^[24,25]

References

- [1] G. G. Brown, B. C. Dian, K. O. Douglass, S. M. Geyer, S. T. Shipman, B. H. Pate, *Rev. Sci. Instrum.* **2008**, *79*, 1–13.
- [2] S. T. Shipman, B. H. Pate, in *Handb. High-Resolution Spectrosc.* (Eds.: F. Merkt, M. Quack), John Wiley & Sons, Ltd, New York, **2011**, pp. 801–828.
- [3] J.-U. Grabow, in *Handb. High-Resolution Spectrosc.* (Eds.: F. Merkt, M. Quack), John Wiley & Sons, Ltd, New York, **2011**, pp. 723–799.
- [4] C. Pérez, S. Lobsiger, N. A. Seifert, D. P. Zaleski, B. Temelso, G. C. Shields, Z. Kisiel, B. H. Pate, *Chem. Phys. Lett.* **2013**, *571*, 1–15.
- [5] N. A. Seifert, A. L. Steber, J. L. Neill, C. Pérez, D. P. Zaleski, B. H. Pate, A. Lesarri, *Phys. Chem. Chem. Phys.* **2013**, *15*, 11468–11477.
- [6] G. T. Fraser, R. D. Suenram, C. L. Lugez, *J. Phys. Chem. A* **2000**, *104*, 1141–1146.
- [7] W. Caminati, J.-U. Grabow, in *Front. Mol. Spectrosc.* (Ed.: J. Laane), Elsevier, Amsterdam, **2009**, pp. 455–552.
- [8] T. A. Halgren, *J. Comput. Chem.* **1996**, *17*, 520–552.
- [9] **2020.**
- [10] W. Kohn, L. J. Sham, *Phys. Rev.* **1965**, *140*, A1133–A1138.
- [11] H. S. Yu, X. He, D. G. Truhlar, *J. Chem. Theory Comput.* **2016**, *12*, 1280–1293.
- [12] Y. Zhao, D. G. Truhlar, *Theor. Chem. Acc.* **2008**, *120*, 215–241.
- [13] A. D. Becke, *J. Chem. Phys.* **1993**, *98*, 5648–5652.
- [14] S. Grimme, J. Antony, S. Ehrlich, H. Krieg, *J. Chem. Phys.* **2010**, *132*, 1–19.
- [15] S. Grimme, S. Ehrlich, L. Goerigk, *J. Comput. Chem.* **2011**, *32*, 1456–1465.
- [16] E. R. Johnson, A. D. Becke, *J. Chem. Phys.* **2006**, *124*, 174104.
- [17] J. Da Chai, M. Head-Gordon, *Phys. Chem. Chem. Phys.* **2008**, *10*, 6615–6620.
- [18] F. Weigend, R. Ahlrichs, *Phys. Chem. Chem. Phys.* **2005**, *7*, 3297–3305.
- [19] M. J. Frisch, G. W. Trucks, H. B. Schlegel, G. E. Scuseria, M. A. Robb, J. R. Cheeseman, G. Scalmani, V. Barone, G. A. Petersson, H. Nakatsuji, et al., **2016**.
- [20] S. Scheiner, *Hydrogen Bonding: A Theoretical Perspective*, Oxford, **1997**.
- [21] B. Jeziorski, R. Moszynski, K. Szalewicz, *Chem. Rev.* **1994**, *94*, 1887–1930.
- [22] R. M. Parrish, L. A. Burns, D. G. A. Smith, A. C. Simmonett, A. E. DePrince, E. G. Hohenstein, U. Bozkaya, A. Y. Sokolov, R. Di Remigio, R. M. Richard, et al., *J. Chem. Theory Comput.* **2017**, *13*, 3185–3197.
- [23] E. G. Hohenstein, C. D. Sherrill, *J. Chem. Phys.* **2010**, *133*, 1–12.
- [24] E. R. Johnson, S. Keinan, P. Mori-Sánchez, J. Contreras-García, A. J. Cohen, W. Yang, *J. Am. Chem. Soc.* **2010**, *132*, 6498–6506.
- [25] J. Contreras-García, E. R. Johnson, S. Keinan, R. Chaudret, J. P. Piquemal, D. N. Beratan, W. Yang, *J. Chem. Theory Comput.* **2011**, *7*, 625–632.

Figure S1. Microwave spectrum of cyclohexanol in the region 2-8 GHz, with x 10 and x 20 expansions of the vertical axis (10^6 averages).

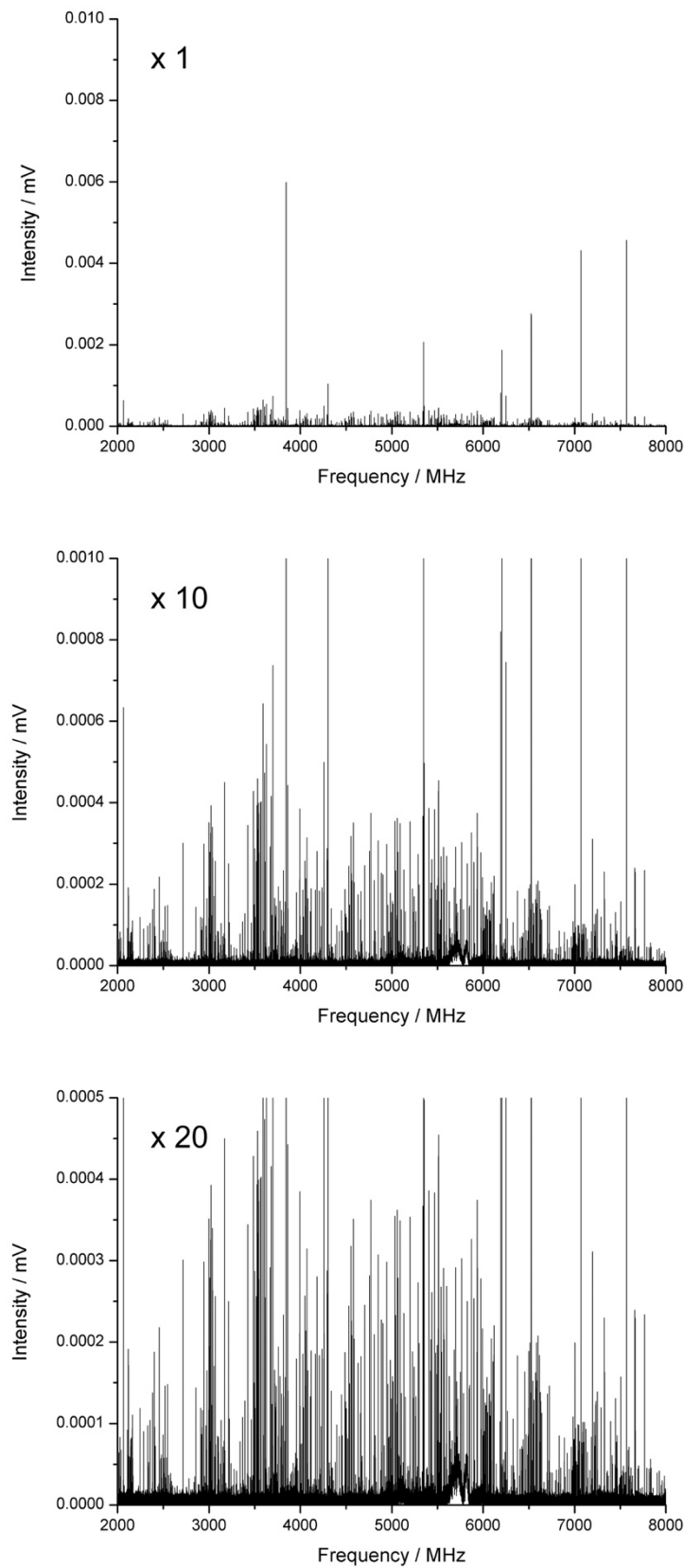


Figure S2. Horizontal expansions of the microwave spectrum of cyclohexanol (x 20).

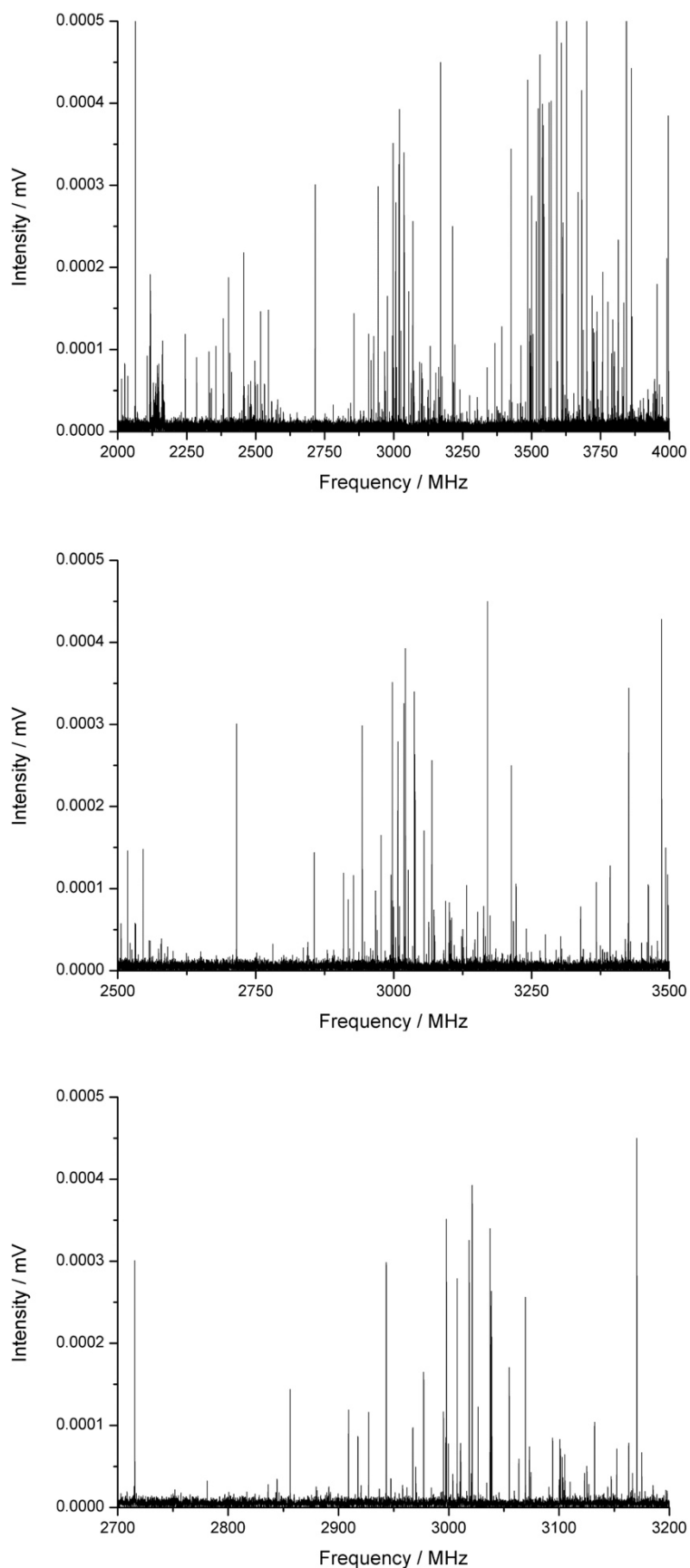


Figure S3. Isomer I (=AT(2)EG-) structure according to B3LYP-D3(BJ)/def2TZVP DFT calculations (rotatable 3D figure in pdf file; atomic coordinates collected in Table S11).

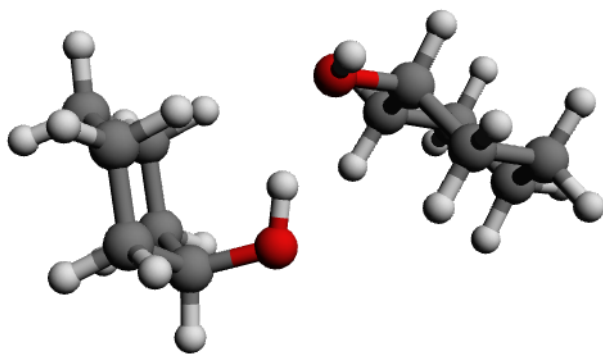


Figure S4. Isomer II (=EG-(2)EG-) structure according to B3LYP-D3(BJ)/def2TZVP DFT calculations (rotatable 3D figure in pdf file; atomic coordinates collected in Table S12).

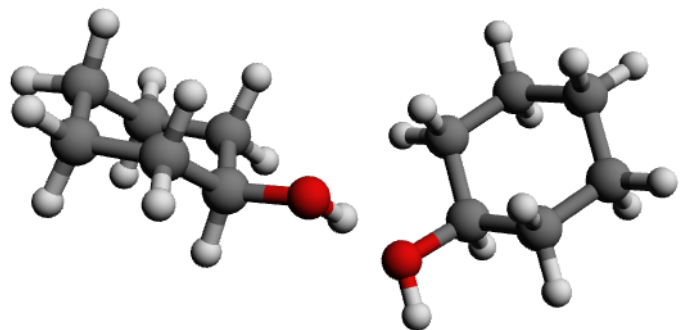


Figure S5. Isomer III (=EG-(1)AG-) structure according to B3LYP-D3(BJ)/def2TZVP DFT calculations (rotatable 3D figure in pdf file; atomic coordinates collected in Table S13).

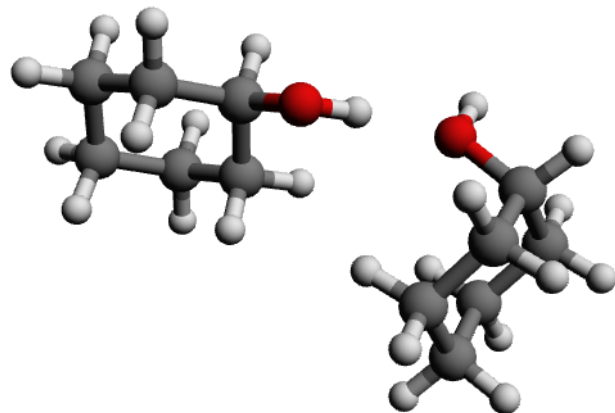


Figure S6. Isomer IV (=EG-(1)AG+) structure according to B3LYP-D3(BJ)/def2TZVP DFT calculations (rotatable 3D figure in pdf file; atomic coordinates collected in Table S14).

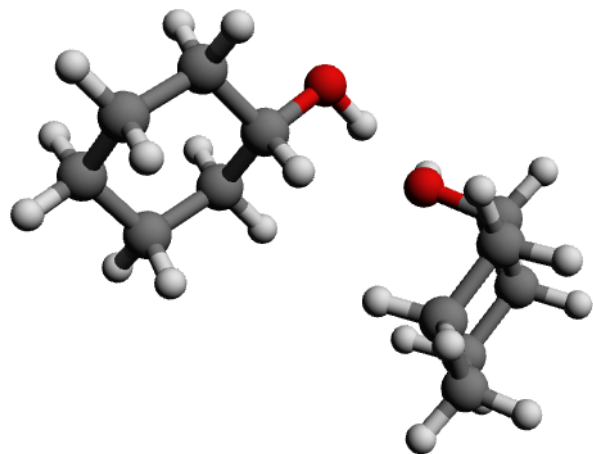


Figure S7. Isomer V (=AG-(1)EG+) structure according to B3LYP-D3(BJ)/def2TZVP DFT calculations (rotatable 3D figure in pdf file; atomic coordinates collected in Table S15).

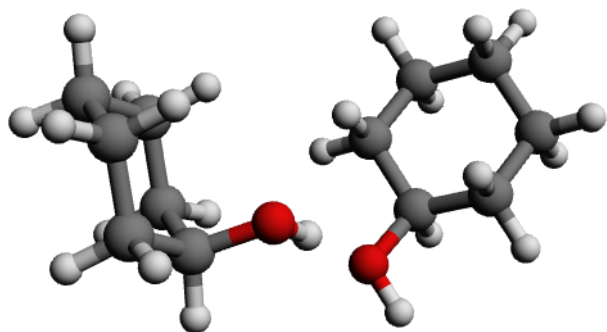


Figure S8. Isomer VI (=EG-(1)EG+) structure according to B3LYP-D3(BJ)/def2TZVP DFT calculations (rotatable 3D figure in pdf file; atomic coordinates collected in Table S16).

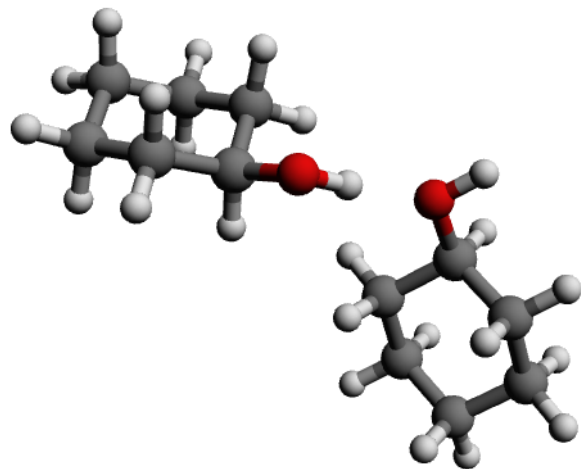


Figure S9. Relative stability of the cyclohexanol monomer as a function of temperature (M06-2X/6-311++G(d,p)).

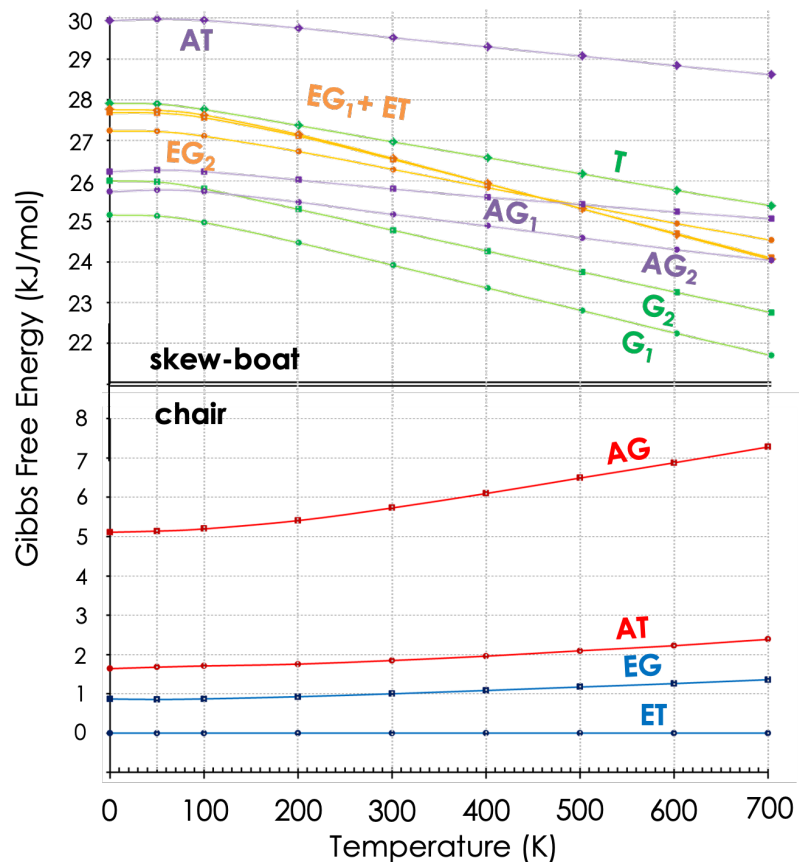


Figure S10. Equatorial-to-axial estimated interconversion barriers for the cyclohexanol monomer starting from an equatorial gauche (EG) geometry and using six different interconversion paths. The reaction barriers are estimations, since no transition-state calculation has been performed. The calculated conformational stabilities gave barrier heights of 47-51 kJ mol⁻¹ using M06-2X/6-311++G(d,p). Similar barriers of 49-54 kJ mol⁻¹ are obtained when starting from an equatorial trans (ET) geometry (not shown).

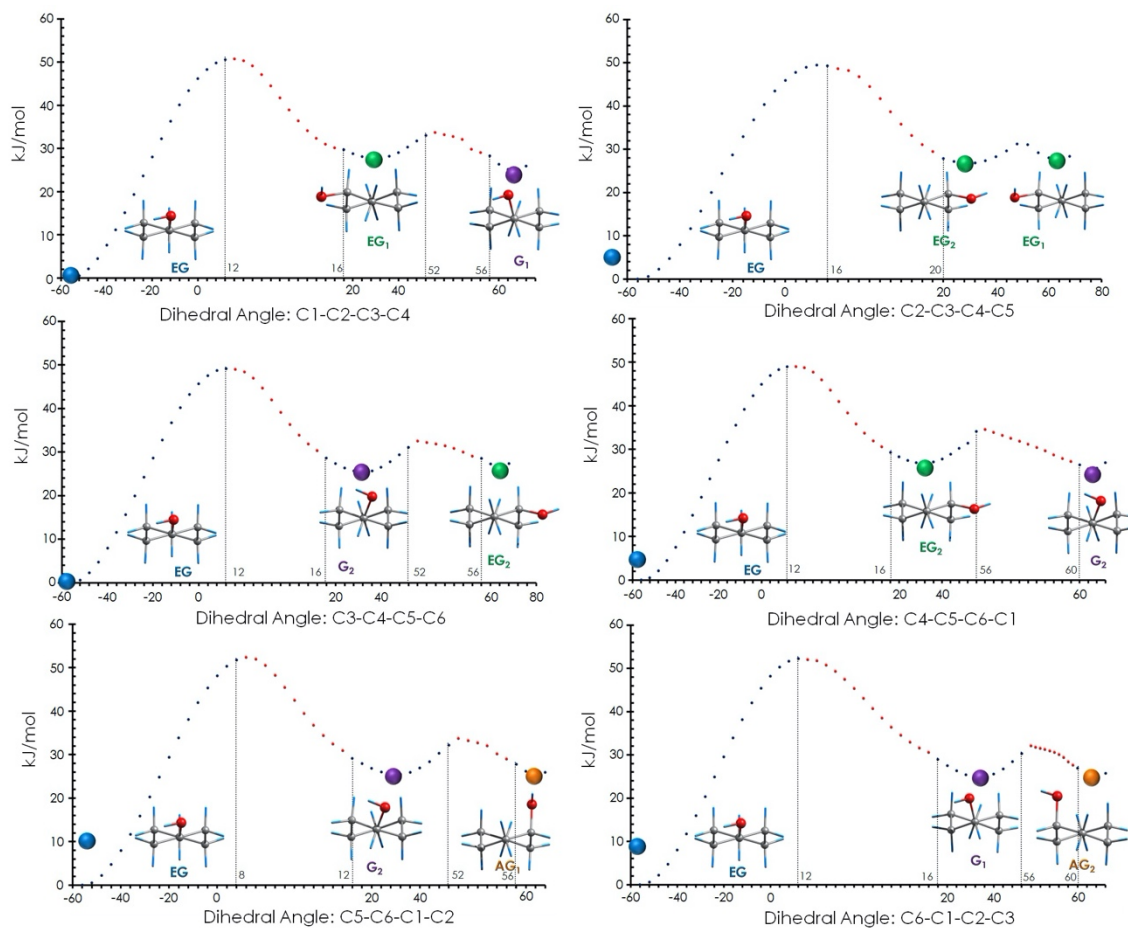


Figure S11. Equatorial-to-axial estimated interconversion barriers for the cyclohexanol dimer starting from the six observed dimer geometries. The reaction barriers are estimations, since no transition-state calculation has been performed. Each interconversion barrier is the average over six interconversion paths using as inversion coordinate the dihedrals C1-C2-C3-C4, C2-C3-C4-C5, C3-C4-C5-C6, C4-C5-C6-C1, C5-C6-C1-C2 and C6-C1-C2-C3. The conformational stabilities were calculated with M06-2X/6-311++G(d,p) and gave barriers heights of 44-51 kJ mol⁻¹.

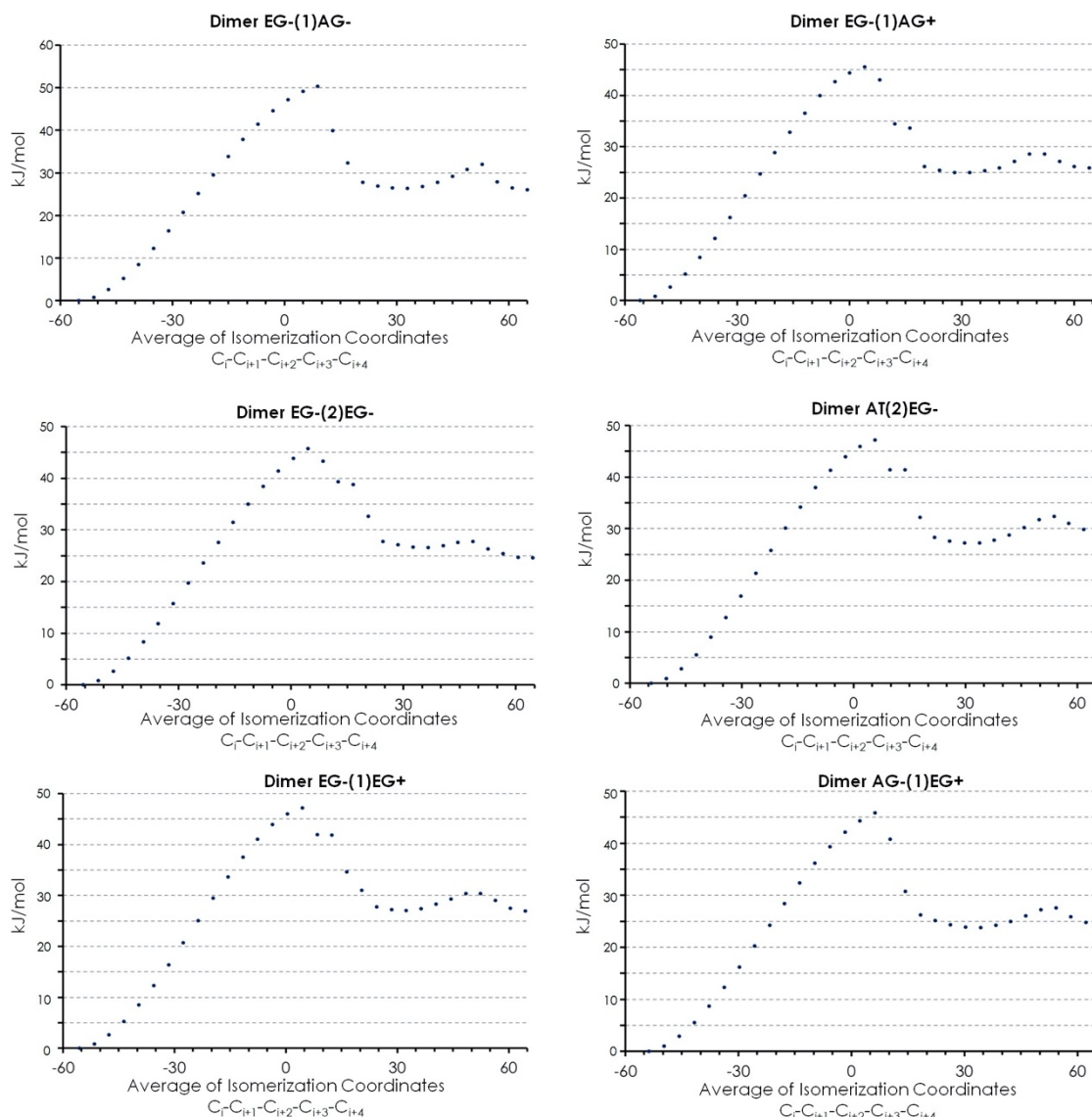


Figure S12. Reduced electronic density gradient s ($= \frac{1}{2(3\pi^2)^{1/3}} \frac{|\nabla\rho|}{\rho^{4/3}}$) vs. the signed electronic density ($= \text{sign}(\lambda_2) \rho$) and NCIPlot for isomer I (=AT(2)EG-) of the cyclohexanol dimer. The plot minimum at negative coordinates indicates a bond critical point and the presence of a O-H \cdots O hydrogen bond interaction. Minima close to the origin denote weak interactions, while the positive minimum is indicative of repulsive interactions like ring critical points. The color scale of the molecular drawing corresponds to attractive interactions (blue), weak interactions (green) or repulsive interactions (red).

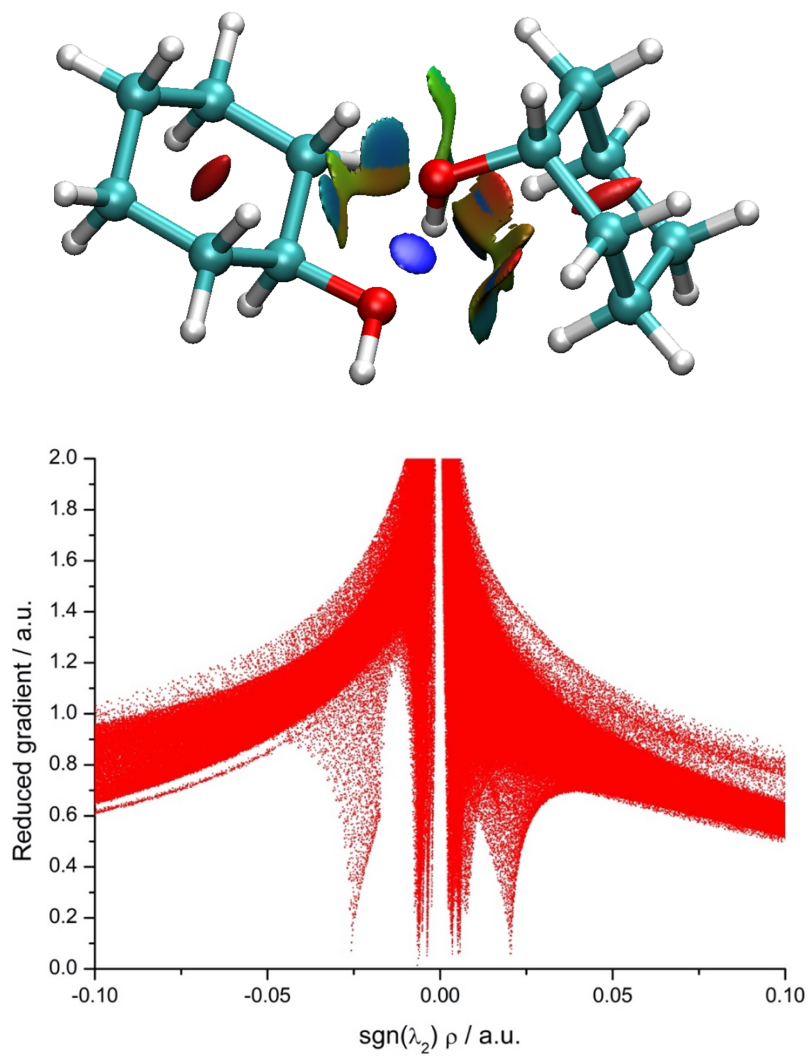


Figure S13. Reduced electronic density gradient s ($= \frac{1}{2(3\pi^2)^{1/3}} \frac{|\nabla\rho|}{\rho^{4/3}}$) vs. the signed electronic density ($= \text{sign}(\lambda_2) \rho$) and NCIPlot drawing for isomer II (=EG-(2)EG-) of the cyclohexanol dimer.

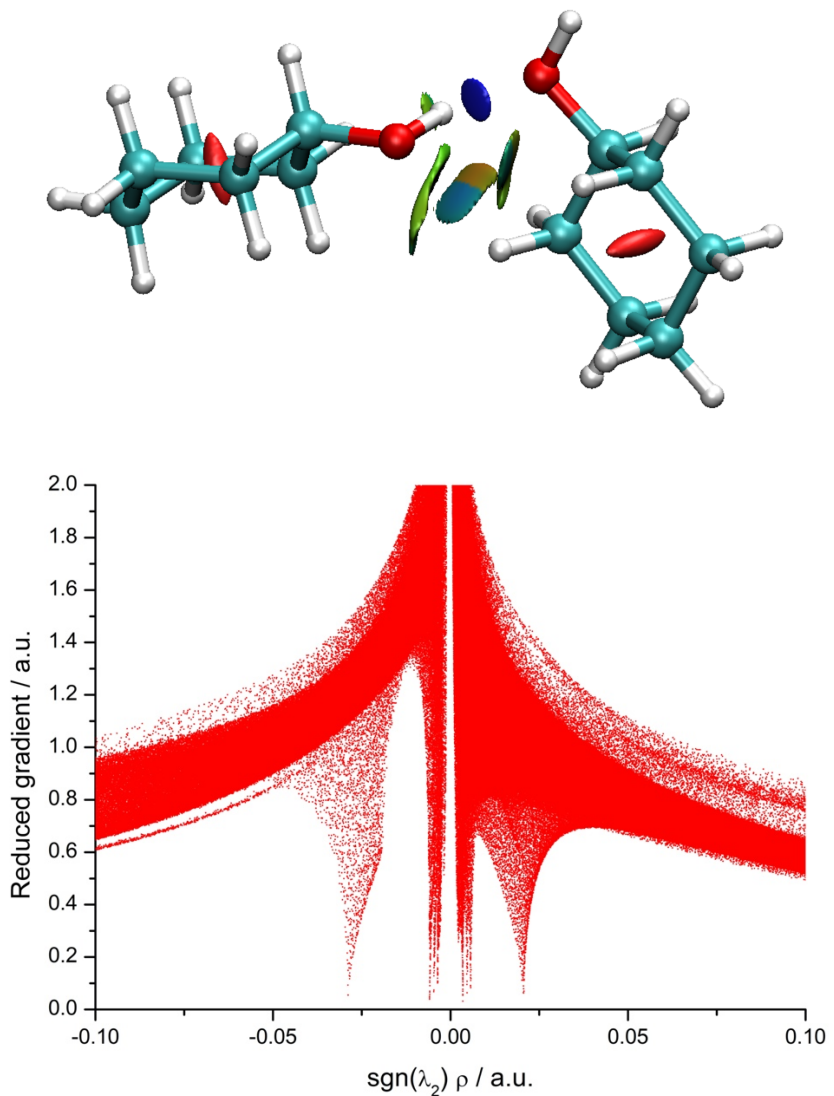


Figure S14. Reduced electronic density gradient s ($= \frac{1}{2(3\pi^2)^{1/3}} \frac{|\nabla\rho|}{\rho^{4/3}}$) vs. the signed electronic density ($= \text{sign}(\lambda_2) \rho$) and NCIPlot drawing for isomer III (=EG-(1)AG-) of the cyclohexanol dimer.

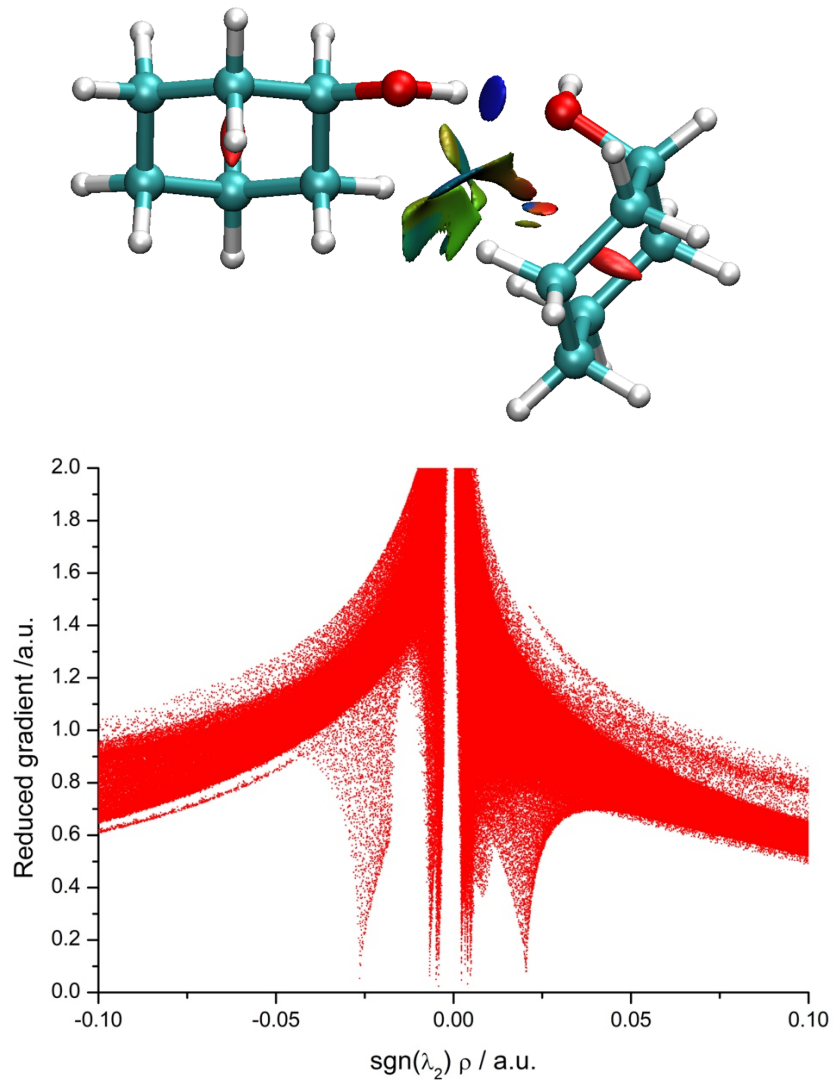


Figure S15. Reduced electronic density gradient s ($= \frac{1}{2(3\pi^2)^{1/3}} \frac{|\nabla\rho|}{\rho^{4/3}}$) vs. the signed electronic density ($= \text{sign}(\lambda_2) \rho$) and NCIPlot drawing for isomer IV (=EG-(1)AG+) of the cyclohexanol dimer.

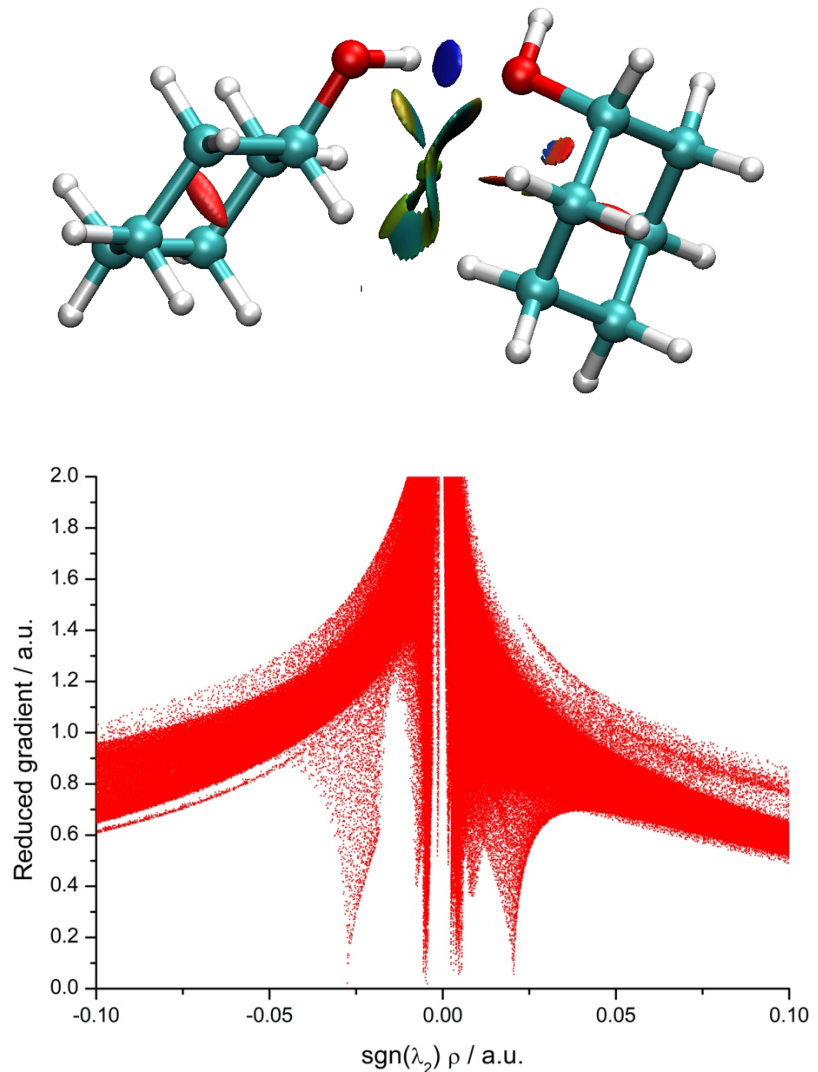


Figure S16. Reduced electronic density gradient s ($= \frac{1}{2(3\pi^2)^{1/3}} \frac{|\nabla\rho|}{\rho^{4/3}}$) vs. the signed electronic density ($= \text{sign}(\lambda_2) \rho$) and NCIPlot drawing for isomer V (=AG-(1)EG+) of the cyclohexanol dimer.

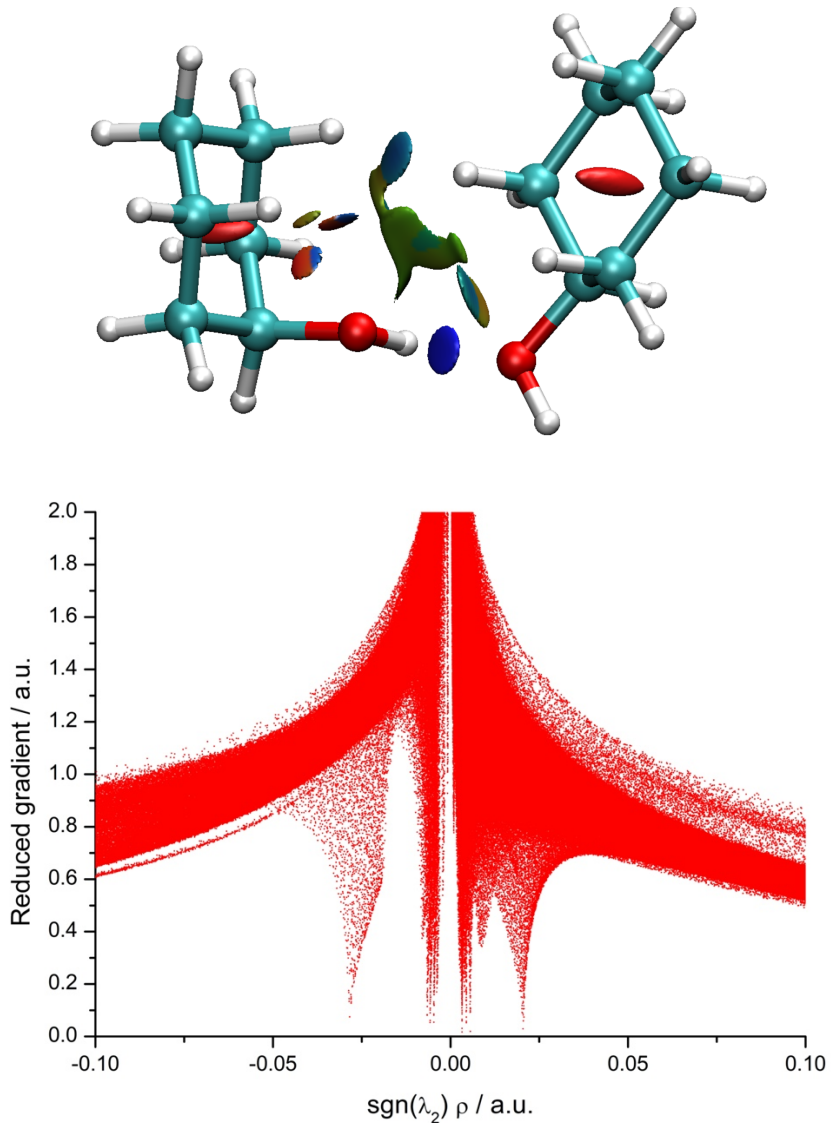


Figure S17. Reduced electronic density gradient s ($= \frac{1}{2(3\pi^2)^{1/3}} \frac{|\nabla\rho|}{\rho^{4/3}}$) vs. the signed electronic density ($= \text{sign}(\lambda_2) \rho$) and NCIPlot drawing for isomer VI (=EG-(1)EG+) of the cyclohexanol dimer.

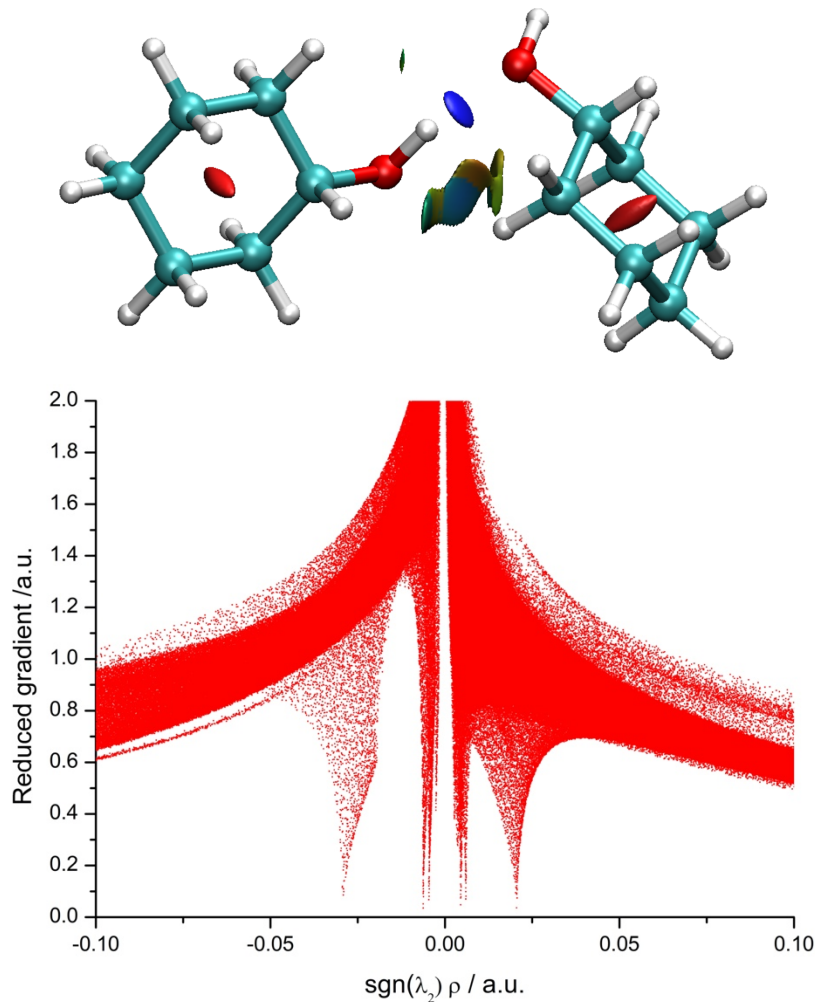


Table S1. Measured rotational transitions of the isomer I (= AT(2)EG-) of the cyclohexanol dimer, residuals according to fit of Table 1 and assumed experimental uncertainties (all values in MHz).

J'	K_{+1}'	K_{+1}'	J''	K_{-1}''	K_{+1}''	Frequency	Residuals	Uncertainty
4	1	4	3	1	3	2458.6880	0.0160	0.020
4	0	4	3	0	3	2481.3087	-0.0568	0.020
4	2	3	3	2	2	2482.4271	-0.0066	0.020
4	2	2	3	2	1	2483.5834	-0.0017	0.020
4	1	3	3	1	2	2505.8997	-0.0045	0.020
5	1	5	4	1	4	3073.1103	-0.0086	0.020
5	0	5	4	0	4	3100.8516	0.0167	0.020
5	2	4	4	2	3	3102.8900	0.0023	0.020
5	4	2	4	4	1	3103.4252	0.0018	0.020
5	3	2	4	3	1	3103.5683	0.0113	0.020
5	2	3	4	2	2	3105.1908	0.0023	0.020
5	1	4	4	1	3	3132.1428	-0.0055	0.020
6	1	6	5	1	5	3687.4327	0.0103	0.020
6	0	6	5	0	5	3719.7146	-0.0128	0.020
6	2	5	5	2	4	3723.2432	0.0046	0.020
6	4	3	5	4	2	3724.1611	-0.0159	0.020
6	3	4	5	3	3	3724.3995	0.0165	0.020
6	3	3	5	3	2	3724.3995	-0.0227	0.020
6	2	4	5	2	3	3727.2606	0.0021	0.020
6	1	5	5	1	4	3758.2431	0.0093	0.020
7	1	7	6	1	6	4301.5524	-0.0050	0.020
7	0	7	6	0	6	4337.9113	-0.0242	0.020
7	2	6	6	2	5	4343.4784	0.0123	0.020
7	2	5	6	2	4	4349.8800	-0.0008	0.020
7	1	6	6	1	5	4384.1289	0.0038	0.020
8	1	8	7	1	7	4915.5053	0.0041	0.020
8	0	8	7	0	7	4955.3570	-0.0024	0.020
8	2	7	7	2	6	4963.5587	0.0091	0.020
8	2	6	7	2	5	4973.1431	0.0097	0.020
8	1	7	7	1	6	5009.7762	-0.0081	0.020
9	1	9	8	1	8	5529.2317	-0.0012	0.020
9	0	9	8	0	8	5571.9206	0.0093	0.020
9	2	8	8	2	7	5583.4720	0.0031	0.020
9	2	7	8	2	6	5597.0857	0.0042	0.020
9	1	8	8	1	7	5635.1970	0.0256	0.020
10	1	10	9	1	9	6142.7315	-0.0032	0.020
10	0	10	9	0	9	6187.5185	-0.0012	0.020
10	2	9	9	2	8	6203.2065	0.0030	0.020
10	6	4	9	6	3	6206.9735	-0.0056	0.020
10	5	6	9	5	5	6207.1881	0.0010	0.020
10	5	5	9	5	4	6207.1881	0.0009	0.020
10	4	6	9	4	5	6207.6411	0.0062	0.020
10	3	8	9	3	7	6208.4637	0.0128	0.020
10	3	7	9	3	6	6209.0001	-0.0049	0.020
10	2	8	9	2	7	6221.7674	-0.0067	0.020
10	1	9	9	1	8	6260.2602	0.0172	0.020
11	1	11	10	1	10	6755.9930	0.0019	0.020
11	0	11	10	0	10	6802.1390	0.0035	0.020
11	2	10	10	2	9	6822.7384	0.0047	0.020

11	5	7	10	5	6	6828.0432	0.0066	0.020
11	5	6	10	5	5	6828.0432	0.0065	0.020
11	4	8	10	4	7	6828.6273	-0.0034	0.020
11	4	7	10	4	6	6828.6273	-0.0156	0.020
11	3	9	10	3	8	6829.6406	-0.0145	0.020
11	3	8	10	3	7	6830.5466	-0.0076	0.020
11	2	9	10	2	8	6847.2240	-0.0141	0.020
11	1	10	10	1	9	6884.9181	-0.0345	0.020
12	1	12	11	1	11	7369.0041	0.0147	0.020
12	0	12	11	0	11	7415.7342	-0.0008	0.020
12	2	11	11	2	10	7442.0318	-0.0075	0.020
12	7	6	11	7	5	7448.3261	-0.0200	0.020
12	6	6	11	6	5	7448.5645	0.0233	0.020
12	5	8	11	5	7	7448.9341	0.0106	0.020
12	5	7	11	5	6	7448.9341	0.0105	0.020
12	4	9	11	4	8	7449.7089	0.0090	0.020
12	4	8	11	4	7	7449.7089	-0.0137	0.020
12	3	10	11	3	9	7450.9487	0.0190	0.020
12	3	9	11	3	8	7452.3196	-0.0053	0.020
12	2	10	11	2	9	7473.4793	0.0052	0.020
12	1	11	11	1	10	7509.2541	0.0035	0.020
13	1	13	12	1	12	7981.7052	-0.0149	0.020

Table S2. Measured rotational transitions of the isomer II (= EG-(2)EG-) of the cyclohexanol dimer, residuals according to fit of Table 1 and assumed experimental uncertainties (all values in MHz).

J'	K_1'	K_{+1}'	J''	K_1''	K_{+1}''	Frequency	Residuals	Uncertainty
4	1	4	3	1	3	2014.2675	0.0071	0.020
4	0	4	3	0	3	2025.2824	0.0006	0.020
4	2	3	3	2	2	2025.5089	-0.0005	0.020
4	2	2	3	2	1	2025.7473	0.0070	0.020
4	1	3	3	1	2	2036.6669	-0.0129	0.020
5	1	5	4	1	4	2517.7727	0.0007	0.020
5	0	5	4	0	4	2531.4103	-0.0082	0.020
5	2	4	4	2	3	2531.8275	-0.0198	0.020
5	3	3	4	3	2	2531.9944	-0.0061	0.020
5	3	2	4	3	1	2531.9944	-0.0073	0.020
5	2	3	4	2	2	2532.3044	-0.0044	0.020
5	1	4	4	1	3	2545.7870	-0.0084	0.020
3	1	2	2	0	2	2556.7423	0.0063	0.020
9	2	8	9	1	8	2937.0445	-0.0091	0.020
8	2	7	8	1	7	2961.9951	0.0090	0.020
7	2	6	7	1	6	2984.2157	0.0191	0.020
6	2	5	6	1	5	3003.6707	0.0035	0.020
5	2	4	5	1	4	3020.3839	0.0010	0.020
6	1	6	5	1	5	3021.2541	0.0059	0.020
4	2	3	4	1	3	3034.3433	0.0122	0.020
6	0	6	5	0	5	3037.4309	-0.0021	0.020
6	2	5	5	2	4	3038.1580	-0.0008	0.020
6	3	4	5	3	3	3038.4084	-0.0074	0.020
6	3	3	5	3	2	3038.4084	-0.0107	0.020
6	2	4	5	2	3	3038.9687	0.0024	0.020
6	1	5	5	1	4	3054.8712	-0.0033	0.020
4	1	3	3	0	3	3074.3739	0.0052	0.020
4	2	2	4	1	4	3090.7294	0.0030	0.020
5	2	3	5	1	5	3105.1895	-0.0737	0.020
6	2	4	6	1	6	3122.9637	-0.0176	0.020
7	2	5	7	1	7	3144.0280	-0.0010	0.020
10	2	8	10	1	10	3228.9648	-0.0222	0.020
9	0	9	8	1	7	3429.0818	-0.0136	0.020
7	1	7	6	1	6	3524.6759	-0.0064	0.020
7	0	7	6	0	6	3543.3084	0.0072	0.020
7	2	6	6	2	5	3544.4409	0.0020	0.020
7	3	5	6	3	4	3544.8462	0.0072	0.020
7	3	4	6	3	3	3544.8462	-0.0002	0.020
7	2	5	6	2	4	3545.7164	-0.0137	0.020
7	1	6	6	1	5	3563.9078	-0.0017	0.020
5	1	4	4	0	4	3594.8784	-0.0040	0.020
10	0	10	9	1	8	3907.0762	0.0058	0.020
8	1	8	7	1	7	4028.0739	0.0060	0.020
8	0	8	7	0	7	4048.9951	-0.0037	0.020
8	2	7	7	2	6	4050.6879	0.0059	0.020
8	3	6	7	3	5	4051.2720	0.0013	0.020
8	3	5	7	3	4	4051.2720	-0.0136	0.020
8	2	6	7	2	5	4052.6310	0.0135	0.020
8	1	7	7	1	6	4072.8847	-0.0077	0.020

2	2	1	1	1	1	4077.9273	0.0675	0.020
6	1	5	5	0	5	4118.3274	-0.0110	0.020
9	1	9	8	1	8	4531.4003	0.0020	0.020
9	0	9	8	0	8	4554.5031	0.0003	0.020
9	2	8	8	2	7	4556.8873	0.0043	0.020
9	4	6	8	4	5	4557.6145	-0.0056	0.020
9	4	5	8	4	4	4557.6145	-0.0057	0.020
9	3	7	8	3	6	4557.7337	0.0220	0.020
9	3	6	8	3	5	4557.7337	-0.0054	0.020
9	2	7	8	2	6	4559.6530	0.0079	0.020
9	1	8	8	1	7	4581.8259	0.0105	0.020
7	1	6	6	0	6	4644.8162	0.0013	0.020
10	1	10	9	1	9	5034.6790	0.0114	0.020
10	0	10	9	0	9	5059.7846	-0.0056	0.020
10	2	9	9	2	8	5063.0390	0.0023	0.020
10	4	7	9	4	6	5064.0284	0.0022	0.020
10	4	6	9	4	5	5064.0284	0.0020	0.020
10	3	8	9	3	7	5064.1834	0.0210	0.020
10	3	7	9	3	6	5064.1834	-0.0259	0.020
10	2	8	9	2	7	5066.8299	0.0008	0.020
10	1	9	9	1	8	5090.6718	0.0018	0.020
8	1	7	7	0	7	5174.4045	-0.0017	0.020
11	1	11	10	1	10	5537.8624	-0.0073	0.020
11	0	11	10	0	10	5564.8395	0.0000	0.020
5	2	3	4	1	3	5566.9734	-0.0126	0.020
11	2	10	10	2	9	5569.1430	0.0053	0.020
11	4	8	10	4	7	5570.4424	0.0091	0.020
11	3	9	10	3	8	5570.5974	-0.0254	0.020
11	3	8	10	3	7	5570.7047	0.0054	0.020
11	2	9	10	2	8	5574.1736	-0.0108	0.020
11	1	10	10	1	9	5599.4580	0.0102	0.020
5	2	4	4	1	4	5622.2032	-0.0242	0.020
9	1	8	8	0	8	5707.2353	0.0125	0.020
12	1	12	11	1	11	6041.0100	0.0107	0.020
6	2	4	5	1	4	6060.1432	-0.0136	0.020
12	0	12	11	0	11	6069.6203	-0.0094	0.020
12	2	11	11	2	10	6075.1755	-0.0054	0.020
12	4	9	11	4	8	6076.8444	0.0026	0.020
12	4	8	11	4	7	6076.8444	0.0018	0.020
12	3	10	11	3	9	6077.0709	-0.0222	0.020
12	3	9	11	3	8	6077.2140	0.0021	0.020
12	2	10	11	2	9	6081.7201	-0.0050	0.020
12	1	11	11	1	10	6108.1369	-0.0030	0.020
10	1	9	9	0	9	6243.3801	-0.0098	0.020
13	1	13	12	1	12	6544.0384	-0.0124	0.020
7	2	5	6	1	5	6551.0241	0.0116	0.020
13	0	13	12	0	12	6574.1389	-0.0033	0.020
13	2	12	12	2	11	6581.1722	0.0111	0.020
13	5	9	12	5	8	6583.1511	0.0017	0.020
13	4	9	12	4	8	6583.2584	0.0054	0.020
13	3	11	12	3	10	6583.5683	-0.0044	0.020
13	3	10	12	3	9	6583.7591	0.0083	0.020
13	2	11	12	2	10	6589.4573	-0.0058	0.020
13	1	12	12	1	11	6616.7324	-0.0047	0.020
7	2	6	6	1	6	6665.7991	-0.0059	0.020
11	1	10	10	0	10	6783.0535	0.0060	0.020
8	2	6	7	1	6	7039.7355	0.0151	0.020

14	1	14	13	1	13	7047.0073	-0.0121	0.020
14	0	14	13	0	13	7078.3713	0.0111	0.020
14	2	13	13	2	12	7087.0736	0.0006	0.020
14	5	9	13	5	8	7089.5293	0.0125	0.020
14	4	10	13	4	9	7089.6723	0.0071	0.020
14	3	12	13	3	11	7090.0538	-0.0071	0.020
14	3	11	13	3	10	7090.3161	-0.0036	0.020
14	2	12	13	2	11	7097.3971	-0.0117	0.020
14	1	13	13	1	12	7125.2445	0.0146	0.020
4	3	1	3	2	1	7129.2737	0.0039	0.020
8	2	7	7	1	7	7191.8230	0.0183	0.020
12	1	11	11	0	11	7326.3748	0.0268	0.020
9	2	7	8	1	7	7526.4679	-0.0051	0.020
15	1	15	14	1	14	7549.8926	-0.0078	0.020
15	0	15	14	0	14	7582.2580	-0.0109	0.020
15	2	14	14	2	13	7592.9034	-0.0080	0.020
15	5	10	14	5	9	7595.8717	-0.0060	0.020
15	4	11	14	4	10	7596.0863	0.0070	0.020
15	3	13	14	3	12	7596.5512	-0.0054	0.020
15	3	12	14	3	11	7596.9208	-0.0022	0.020
15	2	13	14	2	12	7605.5635	-0.0062	0.020
15	1	14	14	1	13	7633.6373	0.0290	0.020
9	2	8	8	1	8	7720.6245	0.0047	0.020
4	1	4	3	1	3	2014.2675	0.0071	0.020

Table S3. Measured rotational transitions of the isomer III (= EG-(1)AG-) of the cyclohexanol dimer, residuals according to fit of Table 1 and assumed experimental uncertainties (all values in MHz).

J'	K_{+1}'	K_{+1}'	J''	K_{-1}''	K_{+1}''	Frequency	Residuals	Uncertainty
4	1	4	3	1	3	2285.6518	0.0123	0.020
4	0	4	3	0	3	2330.1965	-0.0131	0.020
4	2	3	3	2	2	2334.6324	-0.0238	0.020
4	3	2	3	3	1	2335.9663	-0.0230	0.020
4	3	1	3	3	0	2335.9663	-0.0591	0.020
4	2	2	3	2	1	2339.4723	0.0028	0.020
4	1	3	3	1	2	2382.4744	-0.0059	0.020
5	1	5	4	1	4	2856.1728	-0.0023	0.020
5	0	5	4	0	4	2909.1733	-0.0021	0.020
5	2	4	4	2	3	2917.7087	0.0030	0.020
5	3	3	4	3	2	2920.3790	-0.0082	0.020
5	3	2	4	3	1	2920.5221	0.0087	0.020
5	2	3	4	2	2	2927.2932	-0.0036	0.020
5	1	4	4	1	3	2977.1478	0.0065	0.020
4	1	4	3	0	3	3126.7784	-0.0087	0.020
6	1	6	5	1	5	3426.1612	0.0010	0.020
6	0	6	5	0	5	3485.8255	-0.0008	0.020
6	2	5	5	2	4	3500.3691	0.0232	0.020
6	4	2	5	4	1	3504.1957	-0.0006	0.020
6	3	4	5	3	3	3505.0302	0.0102	0.020
6	3	3	5	3	2	3505.3521	-0.0036	0.020
6	2	4	5	2	3	3517.0227	0.0019	0.020
6	1	5	5	1	4	3571.1199	-0.0093	0.020
5	1	5	4	0	4	3652.7546	0.0019	0.020
7	1	7	6	1	6	3995.5058	-0.0098	0.020
7	0	7	6	0	6	4059.8194	-0.0041	0.020
7	2	6	6	2	5	4082.5049	0.0089	0.020
7	3	5	6	3	4	4089.8840	-0.0192	0.020
7	3	4	6	3	3	4090.6469	-0.0107	0.020
7	2	5	6	2	4	4108.8979	0.0024	0.020
7	1	6	6	1	5	4164.2827	0.0068	0.020
6	1	6	5	0	5	4169.7425	0.0051	0.020
8	1	8	7	1	7	4564.1829	0.0041	0.020
8	0	8	7	0	7	4630.9403	-0.0041	0.020
9	0	9	8	1	8	4646.2587	-0.0254	0.020
8	2	7	7	2	6	4664.0924	0.0164	0.020
8	3	6	7	3	5	4675.0359	-0.0012	0.020
8	3	5	7	3	4	4676.5498	0.0077	0.020
7	1	7	6	0	6	4679.4228	-0.0038	0.020
8	2	6	7	2	5	4703.0501	-0.0076	0.020
8	1	7	7	1	6	4756.4083	0.0140	0.020
9	1	9	8	1	8	5132.1090	0.0058	0.020
8	1	8	7	0	7	5183.7863	0.0044	0.020
9	0	9	8	0	8	5199.1286	0.0070	0.020
9	2	8	8	2	7	5245.0123	0.0049	0.020
9	3	7	8	3	6	5260.4142	0.0095	0.020
9	3	6	8	3	5	5263.1560	0.0028	0.020
10	0	10	9	1	9	5278.6533	0.0061	0.020
9	2	7	8	2	6	5299.4792	-0.0080	0.020

9	1	8	8	1	7	5347.2702	-0.0063	0.020
9	1	9	8	0	8	5684.9193	-0.0213	0.020
10	1	10	9	1	9	5699.2602	-0.0007	0.020
10	0	10	9	0	9	5764.4678	0.0015	0.020
10	2	9	9	2	8	5825.2408	0.0268	0.020
10	3	8	9	3	7	5845.9833	0.0123	0.020
10	3	7	9	3	6	5850.6444	-0.0136	0.020
10	2	8	9	2	7	5897.9825	0.0005	0.020
11	0	11	10	1	10	5906.6490	-0.0011	0.020
10	1	9	9	1	8	5936.7017	0.0095	0.020
10	1	10	9	0	9	6185.0747	-0.0053	0.020
11	1	11	10	1	10	6265.6485	0.0070	0.020
11	0	11	10	0	10	6327.2559	-0.0080	0.020
11	2	10	10	2	9	6404.6348	0.0122	0.020
11	6	6	10	6	5	6425.1866	0.0198	0.020
11	5	6	10	5	5	6426.4979	-0.0089	0.020
11	4	8	10	4	7	6429.0370	0.0028	0.020
11	4	7	10	4	6	6429.2397	-0.0059	0.020
11	3	9	10	3	8	6431.6954	0.0118	0.020
11	3	8	10	3	7	6439.2533	0.0072	0.020
11	2	9	10	2	8	6498.1428	-0.0187	0.020
11	1	10	10	1	9	6524.3927	0.0052	0.020
12	0	12	11	1	11	6528.9346	-0.0114	0.020
12	1	12	11	1	11	6831.2619	0.0108	0.020
12	0	12	11	0	11	6887.9460	0.0086	0.020
12	2	11	11	2	10	6983.1586	-0.0053	0.020
12	8	5	11	8	4	7008.2403	-0.0090	0.020
12	7	5	11	7	4	7008.8483	0.0056	0.020
12	6	7	11	6	6	7009.8496	0.0144	0.020
12	5	7	11	5	6	7011.5901	-0.0007	0.020
12	4	9	11	4	8	7014.8207	-0.0075	0.020
12	4	8	11	4	7	7015.2260	0.0023	0.020
12	3	10	11	3	9	7017.4791	0.0057	0.020
12	3	9	11	3	8	7029.1377	0.0112	0.020
12	2	10	11	2	9	7099.4952	-0.0075	0.020
12	1	11	11	1	10	7110.0929	0.0039	0.020
12	1	12	11	0	11	7190.2375	-0.0048	0.020
13	1	13	12	1	12	7396.1004	-0.0109	0.020
13	0	13	12	0	12	7446.9909	0.0062	0.020
13	2	12	12	2	11	7560.7764	0.0019	0.020
13	9	5	12	9	4	7592.1166	-0.0056	0.020
13	8	5	12	8	4	7592.6054	0.0052	0.020
13	7	7	12	7	6	7593.3683	-0.0042	0.020
13	6	7	12	6	6	7594.6439	-0.0066	0.020
13	4	10	12	4	9	7600.9381	0.0002	0.020
13	4	9	12	4	8	7601.6295	-0.0085	0.020
13	3	11	12	3	10	7603.2627	0.0067	0.020
13	3	10	12	3	9	7620.5123	-0.0091	0.020
13	1	12	12	1	11	7693.5043	-0.0052	0.020
13	2	11	12	2	10	7701.3960	-0.0035	0.020
14	1	14	13	1	13	7960.2595	0.0022	0.020
14	0	14	13	0	13	8004.9034	-0.0054	0.020

Table S4. Measured rotational transitions of the isomer IV (= EG-(1)AG+) of the cyclohexanol dimer, residuals according to fit of Table 1 and assumed experimental uncertainties (all values in MHz).

J'	K_{+1}'	K_{+1}''	J''	K_{-1}''	K_{+1}'''	Frequency	Residuals	Uncertainty
4	1	4	3	1	3	2355.4332	-0.0026	0.020
4	0	4	3	0	3	2401.5434	0.0115	0.020
4	2	3	3	2	2	2406.6218	0.0089	0.020
4	3	2	3	3	1	2408.1476	0.0148	0.020
4	3	1	3	3	0	2408.1476	-0.0303	0.020
4	2	2	3	2	1	2412.1054	-0.0102	0.020
4	1	3	3	1	2	2456.4275	-0.0017	0.020
5	1	5	4	1	4	2943.3030	0.0033	0.020
5	0	5	4	0	4	2997.8175	-0.0055	0.020
5	2	4	4	2	3	3007.5689	0.0050	0.020
5	4	2	4	4	1	3010.0484	0.0044	0.020
5	4	1	4	4	0	3010.0484	0.0037	0.020
5	3	3	4	3	2	3010.6087	-0.0118	0.020
5	3	2	4	3	1	3010.7756	-0.0030	0.020
5	2	3	4	2	2	3018.5361	0.0149	0.020
5	1	4	4	1	3	3069.4386	0.0025	0.020
6	0	6	5	0	5	3591.4929	0.0025	0.020
6	2	5	5	2	4	3608.0511	0.0036	0.020
6	5	2	5	5	1	3611.9611	-0.0063	0.020
6	4	2	5	4	1	3612.4499	0.0087	0.020
6	3	4	5	3	3	3613.3797	0.0085	0.020
6	3	3	5	3	2	3613.7970	0.0046	0.020
6	2	4	5	2	3	3627.0769	0.0039	0.020
6	1	5	5	1	4	3681.6629	-0.0040	0.020
7	1	7	6	1	6	4117.0757	0.0036	0.020
7	0	7	6	0	6	4182.1760	-0.0005	0.020
7	2	6	6	2	5	4207.9849	0.0134	0.020
7	3	5	6	3	4	4216.4130	0.0146	0.020
7	3	4	6	3	3	4217.3428	-0.0012	0.020
7	2	5	6	2	4	4238.0257	-0.0057	0.020
7	1	6	6	1	5	4292.9217	-0.0027	0.020
8	1	8	7	1	7	4702.8236	-0.0051	0.020
8	0	8	7	0	7	4769.6763	-0.0015	0.020
8	2	7	7	2	6	4807.2511	0.0062	0.020
8	3	6	7	3	5	4819.6847	-0.0116	0.020
8	3	5	7	3	4	4821.5801	-0.0017	0.020
8	2	6	7	2	5	4851.5017	-0.0001	0.020
8	1	7	7	1	6	4902.9883	0.0004	0.020
9	1	9	8	1	8	5287.7489	-0.0158	0.020
9	0	9	8	0	8	5353.9937	0.0060	0.020
9	2	8	8	2	7	5405.7783	-0.0004	0.020
9	4	6	8	4	5	5420.9894	-0.0105	0.020
9	4	5	8	4	4	5421.0848	0.0174	0.020
9	3	7	8	3	6	5423.2425	0.0038	0.020
9	3	6	8	3	5	5426.6757	-0.0043	0.020
9	2	7	8	2	6	5467.3858	-0.0037	0.020
9	1	8	8	1	7	5511.6125	0.0021	0.020
10	1	10	9	1	9	5871.8637	0.0075	0.020
10	0	10	9	0	9	5935.3070	-0.0084	0.020

10	2	9	9	2	8	6003.4829	-0.0042	0.020
10	7	4	9	7	3	6020.4106	-0.0030	0.020
10	6	5	9	6	4	6021.0782	0.0122	0.020
10	5	5	9	5	4	6022.2226	0.0006	0.020
10	4	7	9	4	6	6024.4042	-0.0102	0.020
10	4	6	9	4	5	6024.5711	0.0109	0.020
10	3	8	9	3	7	6026.9791	0.0015	0.020
10	3	7	9	3	6	6032.8561	0.0160	0.020
10	2	8	9	2	7	6085.3798	0.0001	0.020
10	1	9	9	1	8	6118.5201	0.0025	0.020
11	1	11	10	1	10	6455.0962	-0.0033	0.020
11	0	11	10	0	10	6514.0573	-0.0074	0.020
11	2	10	10	2	9	6600.2815	-0.0068	0.020
11	8	4	10	8	2	6622.2876	-0.0139	0.020
11	8	3	10	8	3	6622.2876	-0.0139	0.020
11	6	6	10	6	5	6623.7181	0.0029	0.020
11	6	5	10	6	4	6623.7181	0.0028	0.020
11	5	7	10	5	6	6625.2678	0.0047	0.020
11	5	6	10	5	5	6625.2678	0.0004	0.020
11	4	8	10	4	7	6628.1408	-0.0106	0.020
11	4	7	10	4	6	6628.4388	-0.0032	0.020
11	3	9	10	3	8	6630.8349	-0.0095	0.020
11	3	8	10	3	7	6640.2882	-0.0012	0.020
11	2	9	10	2	8	6704.9475	-0.0103	0.020
11	1	10	10	1	9	6723.4011	-0.0077	0.020
12	1	12	11	1	11	7037.5182	0.0068	0.020
12	0	12	11	0	11	7090.7691	-0.0016	0.020
12	2	11	11	2	10	7196.1145	0.0084	0.020
12	8	5	11	8	3	7224.6533	-0.0014	0.020
12	8	5	11	8	4	7224.6652	0.0104	0.020
12	8	4	11	8	4	7224.6533	-0.0014	0.020
12	7	6	11	7	4	7225.3566	-0.0039	0.020
12	7	5	11	7	4	7225.3685	0.0079	0.020
12	7	5	11	7	5	7225.3566	-0.0039	0.020
12	6	7	11	6	6	7226.5129	-0.0067	0.020
12	6	6	11	6	5	7226.5129	-0.0068	0.020
12	5	8	11	5	7	7228.5395	-0.0006	0.020
12	5	7	11	5	6	7228.5395	-0.0105	0.020
12	4	9	11	4	8	7232.2112	-0.0175	0.020
12	4	8	11	4	7	7232.7834	0.0116	0.020
12	3	10	11	3	9	7234.7503	-0.0009	0.020
12	3	9	11	3	8	7249.2700	-0.0064	0.020
12	2	10	11	2	9	7325.4568	-0.0132	0.020
12	1	11	11	1	10	7325.9575	-0.0048	0.020
13	1	13	12	1	12	7619.1295	0.0048	0.020
13	0	13	12	0	12	7666.0027	-0.0120	0.020
13	2	12	12	2	11	7790.8985	0.0273	0.020
13	6	8	12	6	7	7829.4985	0.0050	0.020
13	6	7	12	6	6	7829.4985	0.0047	0.020
13	5	9	12	5	8	7832.0973	0.0250	0.020
13	5	8	12	5	7	7832.0973	0.0039	0.020
13	4	10	12	4	9	7836.6511	-0.0059	0.020
13	4	9	12	4	8	7837.6167	-0.0013	0.020
13	3	11	12	3	10	7838.5823	-0.0112	0.020
13	3	10	12	3	9	7860.0639	0.0060	0.020

Table S5. Measured rotational transitions of the isomer V (= AG-(1)EG+) of the cyclohexanol dimer, residuals according to fit of Table 1 and assumed experimental uncertainties (all values in MHz).

J'	K_{-1}'	K_{+1}'	J''	K_{-1}''	K_{+1}''	Frequency ¹	Residuals	Uncertainty
4	1	4	3	1	3	2481.9145	0.0099	0.020
4	0	4	3	0	3	2525.3902	-0.0027	0.020
4	2	2	3	2	1	2537.0131	0.0059	0.020
4	1	3	3	1	2	2578.5219	-0.0130	0.020
5	1	5	4	1	4	3101.2795	0.0029	0.020
5	0	5	4	0	4	3152.2415	-0.0063	0.020
5	2	4	4	2	3	3162.9108	-0.0101	0.020
5	4	1	4	4	0	3165.6765	0.0050	0.020
5	3	3	4	3	2	3166.2606	-0.0145	0.020
5	3	2	4	3	1	3166.5228	0.0485	0.020
5	2	3	4	2	2	3174.9271	0.0057	0.020
5	1	4	4	1	3	3221.9314	0.0050	0.020
6	1	6	5	1	5	3719.9530	-0.0102	0.020
6	0	6	5	0	5	3776.2438	-0.0126	0.020
6	2	5	5	2	4	3794.3398	-0.0022	0.020
6	4	2	5	4	1	3799.1797	-0.0179	0.020
6	3	4	5	3	3	3800.1691	0.0031	0.020
6	3	3	5	3	2	3800.6936	-0.0023	0.020
6	2	4	5	2	3	3815.1299	0.0027	0.020
6	1	5	5	1	4	3864.4350	-0.0017	0.020
7	1	7	6	1	6	4337.8875	0.0113	0.020
7	0	7	6	0	6	4397.0869	0.0020	0.020
7	2	6	6	2	5	4425.1250	-0.0066	0.020
7	3	5	6	3	4	4434.3280	0.0060	0.020
7	3	4	6	3	3	4435.4724	-0.0387	0.020
7	2	5	6	2	4	4457.8480	0.0024	0.020
7	1	6	6	1	5	4505.8299	-0.0069	0.020
8	1	8	7	1	7	4954.9398	-0.0108	0.020
8	0	8	7	0	7	5014.6142	0.0108	0.020
8	2	7	7	2	6	5055.1950	0.0070	0.020
8	3	6	7	3	5	5068.7253	0.0019	0.020
8	3	5	7	3	4	5071.0618	-0.0299	0.020
8	2	6	7	2	5	5103.1053	0.0142	0.020
8	1	7	7	1	6	5145.8777	0.0088	0.020
9	1	9	8	1	8	5571.1576	0.0104	0.020
9	0	9	8	0	8	5628.9266	-0.0030	0.020
9	2	8	8	2	7	5684.4186	0.0063	0.020
9	3	7	8	3	6	5703.3610	0.0354	0.020
9	3	6	8	3	5	5707.6406	-0.0004	0.020
9	2	7	8	2	6	5750.6395	0.0120	0.020
9	1	8	8	1	7	5784.2447	0.0012	0.020
10	1	10	9	1	9	6186.4576	0.0065	0.020
10	0	10	9	0	9	6240.4237	-0.0012	0.020
10	2	9	9	2	8	6312.7005	-0.0099	0.020
10	6	4	9	6	3	6332.1197	0.0007	0.020
10	5	5	9	5	4	6333.3356	-0.0028	0.020
10	4	7	9	4	6	6335.6960	0.0156	0.020
10	4	6	9	4	5	6335.8867	-0.0036	0.020
10	3	8	9	3	7	6338.0563	-0.0025	0.020

10	3	7	9	3	6	6345.3877	-0.0059	0.020
10	2	8	9	2	7	6399.9618	-0.0070	0.020
10	1	9	9	1	8	6420.6328	-0.0069	0.020
11	1	11	10	1	10	6800.8634	-0.0080	0.020
11	0	11	10	0	10	6849.6321	-0.0034	0.020
11	2	10	10	2	9	6939.9809	-0.0132	0.020
11	6	6	10	6	5	6965.8017	-0.0055	0.020
11	5	6	10	5	5	6967.4707	0.0134	0.020
11	4	8	10	4	7	6970.5224	-0.0082	0.020
11	4	7	10	4	6	6970.9516	0.0025	0.020
11	3	9	10	3	8	6972.8232	-0.0072	0.020
11	3	8	10	3	7	6984.6130	0.0016	0.020
11	2	9	10	2	8	7050.4405	0.0040	0.020
11	1	10	10	1	9	7054.7201	0.0105	0.020
12	1	12	11	1	11	7414.4348	-0.0034	0.020
12	0	12	11	0	11	7457.2072	0.0155	0.020
12	2	11	11	2	10	7566.1766	-0.0066	0.020
12	4	8	11	4	7	7606.4933	0.0085	0.020
12	3	10	11	3	9	7607.5185	-0.0083	0.020
12	3	9	11	3	8	7625.5668	-0.0033	0.020
4	1	4	3	1	3	2481.9145	0.0099	0.020

Table S6. Measured rotational transitions of the isomer VI (= EG-(1)EG+) of the cyclohexanol dimer, residuals according to fit of Table 1 and assumed experimental uncertainties (all values in MHz).

J'	K_{+1}'	K_{+1}'	J''	K_{-1}''	K_{+1}''	Frequency	Residuals	Uncertainty
4	1	3	3	1	2	2017.9510	-0.0384	0.020
5	1	5	4	1	4	2472.9728	0.0055	0.020
5	0	5	4	0	4	2496.5773	0.0021	0.020
5	2	4	4	2	3	2497.8170	-0.0023	0.020
5	3	3	4	3	2	2498.2343	0.0027	0.020
5	3	2	4	3	1	2498.2343	-0.0036	0.020
5	2	3	4	2	2	2499.1760	-0.0201	0.020
5	1	4	4	1	3	2522.3384	-0.0056	0.020
6	1	6	5	1	5	2967.3476	-0.0112	0.020
6	0	6	5	0	5	2995.1234	0.0055	0.020
6	2	5	5	2	4	2997.2453	0.0054	0.020
6	3	4	5	3	3	2997.9606	0.0095	0.020
6	3	3	5	3	2	2997.9606	-0.0072	0.020
6	2	4	5	2	3	2999.6534	0.0060	0.020
6	1	5	5	1	4	3026.5947	-0.0070	0.020
7	1	7	6	1	6	3461.6498	0.0067	0.020
7	0	7	6	0	6	3493.2404	-0.0021	0.020
7	2	6	6	2	5	3496.5902	0.0078	0.020
7	4	4	6	4	3	3497.5558	0.0090	0.020
7	4	3	6	4	2	3497.5558	0.0089	0.020
7	3	5	6	3	4	3497.7346	0.0269	0.020
7	3	4	6	3	3	3497.7346	-0.0109	0.020
7	1	6	6	1	5	3530.7437	0.0021	0.020
8	1	8	7	1	7	3955.8091	0.0049	0.020
8	0	8	7	0	7	3990.8924	0.0084	0.020
8	2	7	7	2	6	3995.8277	-0.0059	0.020
8	4	5	7	4	4	3997.2582	0.0010	0.020
8	4	4	7	4	3	3997.2582	0.0006	0.020
8	3	6	7	3	5	3997.5324	0.0269	0.020
8	3	5	7	3	4	3997.5682	-0.0129	0.020
8	2	6	7	2	5	4001.5855	-0.0065	0.020
8	1	7	7	1	6	4034.7496	0.0080	0.020
9	1	9	8	1	8	4449.8252	-0.0023	0.020
9	0	9	8	0	8	4487.9842	0.0035	0.020
9	2	8	8	2	7	4494.9818	0.0009	0.020
9	4	5	8	4	4	4497.0084	0.0157	0.020
9	2	7	8	2	6	4503.1715	-0.0115	0.020
9	1	8	8	1	7	4538.5767	-0.0018	0.020
10	1	10	9	1	9	4943.7341	0.0345	0.020
10	0	10	9	0	9	4984.4680	-0.0087	0.020
10	2	9	9	2	8	4994.0048	-0.0062	0.020
10	4	7	9	4	6	4996.7704	0.0167	0.020
10	4	6	9	4	5	4996.7704	0.0148	0.020
10	3	8	9	3	7	4997.2473	0.0118	0.020
10	3	7	9	3	6	4997.4857	0.0128	0.020
10	2	8	9	2	7	5005.2462	0.0029	0.020
10	1	9	9	1	8	5042.2369	0.0085	0.020
11	1	11	10	1	10	5437.3926	-0.0152	0.020
11	0	11	10	0	10	5480.3081	-0.0154	0.020

11	2	10	10	2	9	5492.9204	0.0090	0.020
11	5	7	10	5	6	5496.2464	-0.0199	0.020
11	4	7	10	4	6	5496.5444	-0.0049	0.020
11	3	9	10	3	8	5497.1762	0.0061	0.020
11	3	8	10	3	7	5497.5577	0.0021	0.020
11	2	9	10	2	8	5507.7978	-0.0086	0.020
11	1	10	10	1	9	5545.6587	-0.0065	0.020
12	1	12	11	1	11	5930.9320	-0.0095	0.020
12	0	12	11	0	11	5975.4687	-0.0135	0.020
12	2	11	11	2	10	5991.6573	-0.0116	0.020
12	5	7	11	5	6	5995.9965	0.0085	0.020
12	4	9	11	4	8	5996.3780	0.0074	0.020
12	4	8	11	4	7	5996.3780	0.0005	0.020
12	3	10	11	3	9	5997.1409	-0.0097	0.020
12	3	9	11	3	8	5997.7370	-0.0126	0.020
12	2	10	11	2	9	6010.9096	0.0128	0.020
12	1	11	11	1	10	6048.8660	0.0039	0.020
13	0	13	12	0	12	6469.9510	0.0256	0.020
13	2	12	12	2	11	6490.2762	0.0049	0.020
13	6	8	12	6	7	6495.5440	0.0030	0.020
13	5	8	12	5	7	6495.7228	-0.0026	0.020
13	4	10	12	4	9	6496.2474	0.0163	0.020
13	4	9	12	4	8	6496.2486	0.0051	0.020
13	3	11	12	3	10	6497.1904	0.0152	0.020
13	2	11	12	2	10	6514.5353	0.0088	0.020
13	1	12	12	1	11	6551.7751	-0.0146	0.020
14	1	14	13	1	13	6917.4384	-0.0092	0.020
14	0	14	13	0	13	6963.6560	0.0166	0.020
14	2	13	13	2	12	6988.6900	-0.0155	0.020
14	6	8	13	6	7	6995.2226	-0.0020	0.020
14	5	9	13	5	8	6995.4730	-0.0072	0.020
14	4	10	13	4	9	6996.1286	-0.0222	0.020
14	3	12	13	3	11	6997.2254	-0.0147	0.020
14	3	11	13	3	10	6998.5247	-0.0181	0.020
14	2	12	13	2	11	7018.6950	0.0008	0.020
14	1	13	13	1	12	7054.3982	-0.0193	0.020
15	1	15	14	1	14	7410.3817	-0.0235	0.020
15	0	15	14	0	14	7456.6231	-0.0021	0.020
15	2	14	14	2	13	7486.9738	0.0143	0.020
15	6	10	14	6	9	7494.8893	-0.0249	0.020
15	5	11	14	5	10	7495.2589	0.0055	0.020
15	4	12	14	4	11	7496.0934	0.0242	0.020
15	4	11	14	4	10	7496.0934	-0.0102	0.020
15	3	13	14	3	12	7497.3331	-0.0073	0.020
15	3	12	14	3	11	7499.1809	-0.0009	0.020
15	2	13	14	2	12	7523.3804	-0.0027	0.020
15	1	14	14	1	13	7556.7114	-0.0015	0.020
16	1	16	15	1	15	7903.1462	-0.0122	0.020
16	2	15	15	2	14	7985.0550	0.0340	0.020
16	4	13	15	4	12	7996.0462	-0.0052	0.020
16	4	12	15	4	11	7996.1534	0.0474	0.020
4	1	3	3	1	2	2017.9510	-0.0384	0.020
5	1	5	4	1	4	2472.9728	0.0055	0.020
5	0	5	4	0	4	2496.5773	0.0021	0.020
5	2	4	4	2	3	2497.8170	-0.0023	0.020
5	3	3	4	3	2	2498.2343	0.0027	0.020
5	3	2	4	3	1	2498.2343	-0.0036	0.020

5	2	3	4	2	2	2499.1760	-0.0201	0.020
5	1	4	4	1	3	2522.3384	-0.0056	0.020
6	1	6	5	1	5	2967.3476	-0.0112	0.020

Table S7. Conformational search of the cyclohexanol dimer using the DFT method B3LYP-D3(BJ)/def2-TZVP. For each isomer the table presents the rotational constants (*A*, *B*, *C*), the relative electronic energy (ΔE , including zero-point and BSSE corrections), the relative Gibbs energy (ΔG , at 1 atm and 298 K) and the relative binding (free) energies (*BE*) at temperatures of 0 K and 298 K. The binding free energies are calculated as differences between the Gibbs energy in the complex and the sum of the Gibbs energies in the two monomers, with the monomer structures corresponding to the most similar stable conformation compared with the structure adopted in the complex.

Experiment	Isomer	Prediction	<i>A</i> / MHz	<i>B</i> / MHz	<i>C</i> / MHz	ΔE / kJ mol ⁻¹	ΔG / kJ mol ⁻¹	<i>BE</i> (0 K) / kJ mol ⁻¹	<i>BE</i> (298 K) / kJ mol ⁻¹
V	AG-(1)EG+	B3LYP-7	1030.73	338.33	312.10	0.93	2.39	0.00	0.00
IV	EG+(2)AG-	B3LYP-9	1208.79	307.43	283.36	1.00	4.43	0.07	2.04
I	AT(2)EG-	B3LYP-26	1228.97	318.01	312.71	3.20	8.00	0.33	4.23
	EG-(2)AG+	B3LYP-12	1119.88	331.23	324.09	1.72	6.77	0.79	4.39
	EG+(2)AG+	B3LYP-15	1348.68	285.74	271.18	1.78	2.54	0.85	0.15
	AG+(1)EG-	B3LYP-18	1195.29	314.53	288.54	2.01	7.01	1.08	4.62
	AG+(1)EG+	B3LYP-13	1372.63	266.43	256.42	2.02	2.83	1.09	0.44
	AG+(1)EG+	B3LYP-14	1356.47	266.07	254.74	2.08	2.70	1.15	0.31
	AG+(2)EG+	B3LYP-23	1322.01	278.24	252.27	2.15	3.30	1.22	0.91
	ET(1)AG-	B3LYP-21	1256.98	304.74	296.18	2.55	4.89	1.43	2.58
	EG+(1)AG-	B3LYP-22	1319.55	281.99	274.88	2.37	4.58	1.44	2.19
VI	EG-(1)EG+	B3LYP-1	1315.30	257.32	245.51	0.00	0.24	1.56	0.82
	EG-(2)EG-	B3LYP-3	1001.09	324.35	308.92	0.01	2.85	1.56	3.43
	EG+(2)AG+	B3LYP-19	1304.17	284.03	267.67	2.57	4.01	1.64	1.62
	ET(1)EG+	B3LYP-4	1379.89	268.76	253.14	0.27	0.78	1.64	1.43
II	EG-(2)EG-	B3LYP-2	1270.09	260.21	255.09	0.10	1.68	1.65	2.26
	ET(2)AG-	B3LYP-25	1139.15	303.95	283.57	2.80	3.18	1.68	0.86
	EG+(1)AG+	B3LYP-24	1369.93	271.93	247.80	2.65	3.96	1.72	1.57

	ET(2)AG+	B3LYP-28	1071.43	335.64	318.82	2.95	3.03	1.84	0.71
III	EG-(2)AG-	B3LYP-27	1202.20	301.24	281.64	2.92	3.83	1.99	1.45
	ET(2)ET	B3LYP-5	1323.91	255.81	249.02	1.03	2.39	2.22	3.11
	AG-(2)EG+	B3LYP-29	1657.28	237.05	221.83	3.19	5.13	2.25	2.74
	ET(1)AT	B3LYP-30	1493.45	251.25	242.53	5.39	8.44	2.34	4.74
	EG-(1)EG-	B3LYP-6	1410.87	234.86	225.86	1.02	0.00	2.58	0.58
	EG-(2)EG+	B3LYP-8	1492.06	231.97	222.48	1.12	0.29	2.67	0.87
	ET(2)ET	B3LYP-20	1052.08	321.02	282.13	1.55	1.36	2.74	2.08
	ET(2)EG+	B3LYP-10	1355.35	251.46	240.88	1.40	0.43	2.77	1.08
	EG-(1)EG+	B3LYP-17	1039.16	327.63	286.59	1.49	1.40	3.04	1.98
	ET(1)EG+	B3LYP-16	956.19	351.66	319.50	1.89	3.34	3.26	3.99
	ET(2)EG-	B3LYP-11	1418.17	264.06	251.23	2.08	1.92	3.45	2.57

Table S8. Conformational search of the cyclohexanol dimer using the DFT method MN15-L/def2-TZVP. For each isomer the table presents the rotational constants (*A*, *B*, *C*), the relative electronic energy (ΔE , including zero-point and BSSE corrections), the relative Gibbs energy (ΔG , at 1 atm and 298 K) and the relative binding (free) energies (*BE*) at temperatures of 0 K and 298 K. The binding free energies are calculated as differences between the Gibbs energy in the complex and the sum of the Gibbs energies in the two monomers, with the monomer structures corresponding to the most similar stable conformation compared with the structure adopted in the complex.

Experiment	Isomer	Prediction	<i>A</i> / MHz	<i>B</i> / MHz	<i>C</i> / MHz	ΔE / kJ mol ⁻¹	ΔG / kJ mol ⁻¹	<i>BE</i> (0 K) / kJ mol ⁻¹	<i>BE</i> (298 K) / kJ mol ⁻¹
VI	EG-(1)EG+	MN15L-1	1337.05	267.26	253.69	5.81	5.38	7.19	5.39
II	EG-(2)EG-	MN15L-2	1256.37	265.31	260.87	3.95	3.62	5.33	3.62
	EG-(2)EG-	MN15L-3	959.3	341.45	320.93	0.00	1.11	1.38	1.12
	ET(2)EG-	MN15L-4	1345.36	281.09	266.76	2.99	4.18	3.83	4.14
	ET(1)EG+	MN15L-4b	1345.31	281.01	266.7	2.99	4.15	3.82	4.11
	ET(2)ET	MN15L-5	1348.68	265.02	252.47	6.73	5.67	7.02	5.59
	ET(2)ET	MN15L-5b	967.66	335.89	315.67	4.67	5.46	4.95	5.37
	EG-(2)EG-	MN15L-6	1042.72	310.13	281.41	4.06	0.14	5.44	0.15
	EG+(1)EG+	MN15L-6b	1043.71	309.71	281.21	4.03	0.00	5.41	0.01
	EG-(2)EG-	MN15L-6c	1042.87	310.07	281.37	4.06	0.14	5.44	0.15
V	AG-(1)EG+	MN15L-7	973.58	363.38	327.25	2.31	3.26	2.51	1.43
	EG-(1)EG+	MN15L-8	1156.33	275.1	260.36	4.34	2.64	5.72	2.64
	EG-(2)EG+	MN15L-8b	1372.52	241.63	231.03	6.71	5.13	8.09	5.14
IV	EG-(1)AG+	MN15L-9	1171.87	319.45	290.54	1.54	4.63	1.74	2.79
II	EG+(2)AG-	MN15L-9b	1172.14	319.46	290.56	1.55	4.66	1.75	2.83
	ET(2)EG-	MN15L-10	1267.64	262.71	256.56	5.77	4.62	6.60	4.58
	ET(2)EG-	MN15L-11	1121.3	301.76	287.69	2.63	2.83	3.46	2.79
	EG-(2)AG+	MN15L-12	1084.27	339.63	328.18	1.98	5.89	2.18	4.06

	AG+(2)EG+	MN15L-13	1297.32	280.96	262.1	8.37	6.62	8.57	4.79
	AG-(2)EG-	MN15L-13b	1348.91	286.18	277.17	4.52	5.07	4.72	3.24
	AG+(1)EG+	MN15L-14	1392.81	267.46	253.26	6.93	6.85	7.13	5.02
	EG+(2)AG+	MN15L-15	1296.34	292.23	283.89	2.93	5.25	3.13	3.42
	ET(1)EG+	MN15L-16	911.68	367.08	333.4	4.76	4.92	5.59	4.87
	ET(2)EG-	MN15L-16b	920.89	350.79	311.12	5.27	3.53	6.10	3.49
	EG-(1)EG+	MN15L-17	1100.48	245.66	216.88	19.47	13.70	20.85	13.71
	AG+(1)EG-	MN15L-18	1395.66	272.77	248.17	5.01	4.56	5.21	2.73
	EG+(2)AG+	MN15L-19	1259.13	292.47	283.62	5.45	6.95	5.65	5.11
	ET(2)ET	MN15L-20	1051.98	310.98	272.96	4.95	3.53	5.24	3.44
	ET(2)AG-	MN15L-21	1366.86	284.15	276.57	3.50	4.73	3.15	2.85
	ET(1)AG-	MN15L-21b	1201.62	315.44	310.46	3.14	6.28	2.79	4.40
	EG+(1)AG-	MN15L-22	1302.96	285.51	276.14	5.08	5.48	5.28	3.65
	AG+(2)EG+	MN15L-23	1285.21	284.97	257.76	4.95	3.89	5.15	2.06
	AG+(1)EG+	MN15L-23b	1163.69	309.43	283.58	2.96	1.83	3.17	0.00
	EG+(1)AG+	MN15L-24	1221.05	293.3	275.41	4.02	2.76	4.22	0.93
	EG+(1)AG+	MN15L-24b	1326.44	279.79	253.64	6.08	6.17	6.28	4.34
	ET(2)AG-	MN15L-25	1023.26	346.59	315.8	4.67	5.74	4.32	3.86
I	AT(2)EG-	MN15L-26	1186.92	321.79	318.09	2.27	5.72	0.00	1.41
III	EG-(2)AG-	MN15L-27	1221.03	293.31	275.41	4.02	2.76	4.22	0.93
	ET(1)AG+	MN15L-28	1073.42	332.28	319.59	1.81	2.31	1.46	0.43
	AG-(1)EG+	MN15L-29	1330.49	282.32	269.06	4.39	3.46	4.59	1.63
	ET(1)AT	MN15L-30	1142.23	291.35	286.36	9.15	8.37	6.33	4.02
	ET(1)AT	MN15L-30b	1439.14	260.87	247.31	10.00	9.94	7.18	5.59

Table S9. Conformational search of the cyclohexanol dimer using the DFT method M06-2X-6-311++G(d,p). For each isomer the table presents the rotational constants (A , B , C), the relative electronic energy (ΔE , including zero-point and BSSE corrections), the relative Gibbs energy (ΔG , at 1 atm and 298 K) and the relative binding (free) energies (BE) at temperatures of 0 K and 298 K. The binding free energies are calculated as differences between the Gibbs energy in the complex and the sum of the Gibbs energies in the two monomers, with the monomer structures corresponding to the most similar stable conformation compared with the structure adopted in the complex.

Experiment	Prediction	Prediction	A / MHz	B / MHz	C / MHz	ΔE / kJ mol ⁻¹	ΔG / kJ mol ⁻¹	BE (0 K) / kJ mol ⁻¹	BE (298 K) / kJ mol ⁻¹
VI	EG-(1)EG+	M062X-1	1334.89	264.03	251.56	2.02	1.58	4.73	4.08
II	EG-(2)EG-	M062X-2	1256.64	269.81	265.38	1.24	1.47	3.96	3.96
	EG-(2)EG-	M062X-3	988.7	342.69	323.64	0.20	0.98	2.92	3.48
	ET(2)EG-	M062X-4	1382.92	279	263.23	1.69	3.33	3.53	4.56
	ET(1)EG+	M062X-4b	1372.81	280.03	263.68	2.72	5.35	4.57	6.58
	ET(2)ET	M062X-5	1391.71	263.11	251.26	2.68	3.71	3.66	3.67
	ET(2)ET	M062X-5b	1004.25	332.44	313.73	5.80	12.12	6.78	12.09
	EG-(1)EG-	M062X-6	1145.91	288.27	270.61	1.60	5.17	4.32	7.66
	EG+(2)EG+	M062X-6b	1184.87	278.54	266.98	2.01	1.00	4.73	3.49
	EG-(2)EG-	M062X-6c	1075.53	307.94	285.32	3.42	7.22	6.14	9.72
V	AG-(1)EG+	M062X-7	1021.03	352.56	323.2	2.64	4.26	3.72	4.26
	EG-(1)EG+	M062X-8	1243.04	269.13	255.12	2.51	3.64	5.23	6.13
	EG-(2)EG+	M062X-8b	1411.28	246.74	236.26	3.04	4.53	5.76	7.03
	EG-(1)AG+	M062X-9	1193.44	327.43	299.29	0.96	6.43	2.04	6.43
IV	EG+(2)AG-	M062X-9b	1201.65	325.06	297.31	1.45	8.33	2.53	8.33
	ET(2)EG+	M062X-10	1328.14	262.91	254.13	3.10	2.49	4.95	3.72
	ET(2)EG-	M062X-11	1114.28	310.18	293.63	2.21	3.54	4.06	4.78
	EG-(2)AG+	M062X-12	1115.91	346.44	336.8	2.25	8.42	3.33	8.42

	AG+(1)EG+	M062X-13	1258.40	288.00	269.60	3.36	5.43	4.44	5.43
	AG-(2)EG-	M062X-13b	1457.58	264.73	252.67	3.68	9.70	4.76	9.70
	AG+(1)EG+	M062X-14	1352.03	274.36	261.22	3.14	2.58	4.22	2.58
	EG+(2)AG+	M062X-15	1334.76	300.9	290.20	0.00	3.13	1.08	3.13
	ET(1)EG+	M062X-16	945.49	364.21	330.93	5.45	7.64	7.30	8.88
	ET(2)EG-	M062X-16b	935.60	351.39	313.91	6.02	7.31	7.87	8.54
	EG-(1)EG+	M062X-17	1112.39	255.96	225.56	21.84	27.92	24.55	30.42
	AG+(1)EG-	M062X-18	1397.13	283.09	255.74	2.48	4.37	3.56	4.37
	EG+(2)AG+	M062X-19	1280.46	300.02	289.81	3.89	8.63	4.97	8.63
	ET(2)ET	M062X-20	1079.11	318.42	280.61	3.95	2.37	4.93	2.34
	ET(2)AG-	M062X-21	1416.28	283.61	277.96	2.20	2.26	2.41	1.00
	ET(1)AG-	M062X-21b	1246.81	318.2	311.51	3.19	6.93	3.40	5.67
	EG+(1)AG-	M062X-22	1322.85	287.69	278.90	2.36	5.04	3.44	5.04
	AG+(2)EG+	M062X-23	1300.10	294.00	264.99	1.27	0.94	2.35	0.94
	AG+(2)EG+	M062X-23b	1244.92	303.46	276.25	2.89	2.63	3.97	2.63
	EG+(1)AG+	M062X-24	1273.98	291.65	274.35	2.74	0.00	3.81	0.00
	EG+(1)AG+	M062X-24b	1362.23	284.59	258.36	4.02	7.40	5.10	7.40
	ET(2)AG-	M062X-25	1056.37	348.17	319.61	5.12	10.79	5.33	9.52
I	AT(2)EG-	M062X-26	1221.46	331.00	326.05	2.39	8.48	0.00	4.01
III	EG-(2)AG-	M062X-27	1254.49	296.54	278.11	2.82	3.21	3.90	3.21
	ET(2)AG+	M062X-28	1102.62	337.31	322.02	1.94	2.65	2.15	1.39
	AG-(2)EG+	M062X-29	1487.08	263.62	250.50	1.25	1.31	2.33	1.31
	ET(1)AT	M062X-30	1182.64	293.83	290.24	6.63	9.42	3.37	3.68
	ET(1)AT	M062X-30b	1495.56	259.74	248.44	9.30	19.40	6.04	13.66

Table S10. Comparison of experimental and predicted rotational parameters for the six observed isomers of the cyclohexanol dimer, using the DFT methods B3LYP-D3(BJ) and ωB97XD (def2-TZVP basis set). The relative differences of the predicted rotational constants with the experimental values are shown in square brackets. The complexation energy (E_c) corresponds to the difference between the electronic energy of the dimer and the sum of the monomers in the dimer configuration, including BSSE corrections (see Table S17 for the SAPT2+(3) binding energy calculation).

	Isomer I		Isomer II		Isomer III	
	Experiment	AT(2)EG- ^[d]	Experiment	EG-(2)EG-	Experiment	EG-(1)AG-
A / MHz ^[a]	1218.11(23) ^[b]	1228.97[0.9%]/1222.21[0.3%]	1273.9599(22)	1270.09[-0.3%]/1261.33[-1.0%]	1203.5721(82)	1202.20[-0.1%]/1207.12[0.3%]
B / MHz	316.22133(97)	318.01[0.6%]/327.71[3.6%]	255.99343(18)	260.21[1.6%]/268.84[4.8%]	303.99025(48)	301.24[-0.9%]/307.98[1.3%]
C / MHz	304.41165(91)	312.71[2.7%]/321.73[5.4%]	250.38848(19)	255.09[1.8%]/261.91[4.4%]	279.76964(43)	281.64[0.7%]/285.95[2.2%]
D _J / kHz	0.0583(13)	0.040/0.031	0.05908(57)	0.056/0.039	0.06469(69)	0.051/0.033
D _{JK} / kHz	-0.1976(88)	-0.077/-0.060	-0.4638(99)	-0.428/-0.261	-0.2661(34)	0.032/0.019
D _K / kHz	[0.0]	0.443/0.274	1.45(34)	2.468/1.725	[0.0]	0.253/0.188
d ₁ / kHz	-0.0043(19)	-0.00097/-0.0002	[0.0]	-0.00092/0.00262	-0.01083(87)	-0.0037/-0.0015
d ₂ / kHz	[0.0]	0.00001/-0.00001	[0.0]	-0.00040/-0.00044	[0.0]	-0.00022/-0.00011
μ _a / D	+ ^[c]	1.10/1.10	+	1.83/1.87	+	2.07/2.17
μ _b / D	-	0.12/0.06	-	0.17/0.17	+	1.53/1.44
μ _c / D	-	1.34/1.29	+	1.09/1.14	-	1.89/1.95
ΔE _{ZPE} / kJ mol ⁻¹		3.20/1.99		0.10/0.00		2.92/3.05
ΔG / kJ mol ⁻¹		8.00/9.35		1.68/3.80		3.83/8.16
E _c / kJ mol ⁻¹		-33.85/-36.28		-31.76/-33.39		-30.54/-32.64

^[a]Rotational constants (A, B, C), Watson's S-reduced centrifugal distortion constants (D_J, D_{JK}, D_K, d₁, d₂), electric dipole moment (μ_a, α = a, b, c), electronic energies including zero-point corrections (ΔE_{ZPE}), Gibbs energies (ΔG) and complexation energies including basis set superposition errors (E_c). ^[b]Standard errors in parentheses in units of the last digit. ^[c]A positive sign indicates the selection rules corresponding to the observed transitions. ^[d]Predictions from the B3LYP-D3(BJ)/def2TZVP and ωB97XD/def2TZVP calculations, respectively. The predicted rotational constants are followed by the relative percentage errors in square brackets, defined as (theory-experiment)/theory.

Table S10. Continued.

	Isomer IV		Isomer V		Isomer VI	
	Experiment	EG-(1)AG+ ^[d]	Experiment	AG-(1)EG+	Experiment	EG-(1)EG+
<i>A</i> / MHz ^[a]	1167.877(41) ^[b]	1208.79[3.0%]/1195.20[2.3%]	1039.694(67)	1030.73[-0.9%]/998.54[-4.1%]	1311.72(22)	1315.30[0.3%]/1297.52[-1.1%]
<i>B</i> / MHz	313.51209(51)	307.43[-2.4%]/322.36[2.7%]	328.52277(90)	338.33[2.9%]/374.72[12.3%]	254.73673(31)	257.32[0.3%]/265.01[3.9%]
<i>C</i> / MHz	288.25106(51)	283.36[-1.7%]/293.99[2.0%]	304.34728(85)	312.10[2.5%]/337.26[9.8%]	244.86010(34)	245.51[1.0%]/253.57[3.4%]
<i>D_J</i> / kHz	0.06942(56)	0.061/0.055	0.2037(13)	0.395/0.060	0.06438(54)	0.061/0.102
<i>D_{JK}</i> / kHz	-0.2290(26)	-0.215/-0.233	-0.475(11)	-0.740/-0.040	-0.5107(72)	-0.595/-1.288
<i>D_K</i> / kHz	[0.0]	0.720/0.665	[0.0]	2.150/0.144	[0.0]	3.339/9.721
<i>d₁</i> / kHz	-0.01058(97)	-0.010/-0.009	-0.0286(20)	-0.060/-0.009	[0.0]	-0.0041/0.0062
<i>d₂</i> / kHz	[0.0]	-0.00067/-0.00044	[0.0]	0.0019/-0.0004	[0.0]	-0.00034/-0.00089
μ_a / <i>D</i>	+ ^[c]	2.97/3.00	+	2.12/1.85	+	2.06/2.07
μ_b / <i>D</i>	-	1.11/1.14	-	0.28/0.16	-	0.83/0.82
μ_c / <i>D</i>	-	0.54/0.51	-	0.42/0.18	-	0.85/0.91
ΔE_{ZPE} / kJ mol ⁻¹		1.00/0.30		0.93/0.58		0.00/0.05
ΔG / kJ mol ⁻¹		4.43/7.06		2.39/8.38		0.24/0.00
<i>E_c</i> / kJ mol ⁻¹		-33.10/-35.82		-33.76/-36.28		-31.84/-33.01

^[a]Rotational constants (*A*, *B*, *C*), Watson's S-reduced centrifugal distortion constants (*D_J*, *D_{JK}*, *D_K*, *d₁*, *d₂*), electric dipole moment (μ_α , $\alpha = a, b, c$), electronic energies including zero-point corrections (ΔE_{ZPE}), Gibbs energies (ΔG) and complexation energies including basis set superposition errors (*E_c*). ^[b]Standard errors in parentheses in units of the last digit. ^[c]A positive sign indicates the selection rules corresponding to the observed transitions.

^[d]Predictions from the B3LYP-D3(BJ)/def2TZVP and ωB97XD/def2TZVP calculations, respectively. The predicted rotational constants are followed by the relative percentage errors in square brackets, defined as (theory-experiment)/theory.

Table S11. Atomic coordinates for isomer I (= AT(2)EG-) of the cyclohexanol dimer according to B3LYP-D3(BJ)/def2TZVP DFT calculations (principal axes system).

Atom	<i>a</i> / Å	<i>b</i> / Å	<i>c</i> / Å
C	3.2064	0.7482	0.8834
C	3.1893	1.1349	-0.5973
C	2.1097	0.3848	-1.3841
C	2.2331	-1.1282	-1.1754
C	2.2568	-1.5171	0.3051
C	3.3541	-0.7644	1.0607
H	4.0160	1.2739	1.3956
H	2.2773	1.0748	1.3613
H	4.1641	0.9013	-1.0395
H	3.0302	2.2087	-0.7175
H	2.2336	0.6041	-2.4472
H	1.4092	-1.6241	-1.6938
H	3.1608	-1.4658	-1.6508
H	1.2909	-1.2919	0.7642
H	2.4007	-2.5962	0.4015
H	4.3347	-1.0761	0.6823
H	3.3292	-1.0255	2.1216
O	0.8015	0.8627	-1.0773
H	0.5868	0.7066	-0.1434
C	-3.8039	0.9264	-0.2789
C	-2.4070	1.3230	0.2061
C	-1.8097	0.2409	1.0987
C	-1.7690	-1.1032	0.3900
C	-3.1631	-1.5078	-0.0942
C	-3.7772	-0.4288	-0.9878
H	-4.4869	0.8727	0.5764
H	-4.1980	1.6980	-0.9437
H	-1.7400	1.4697	-0.6478
H	-2.4499	2.2713	0.7524
H	-2.4200	0.1440	2.0069
H	-1.3554	-1.8568	1.0635
H	-1.0911	-1.0191	-0.4636
H	-3.1049	-2.4580	-0.6294
H	-3.8160	-1.6765	0.7695
H	-4.7872	-0.7169	-1.2889
H	-3.1854	-0.3422	-1.9050
O	-0.4614	0.5635	1.4923
H	-0.4671	1.4277	1.9196

Table S12. Atomic coordinates for isomer II (= EG-(2)EG-) of the cyclohexanol dimer according to B3LYP-D3(BJ)/def2TZVP DFT calculations (principal axes system).

Atom	<i>a</i> / Å	<i>b</i> / Å	<i>c</i> / Å
C	4.3040	-0.4265	0.8146
C	2.8871	-0.9266	1.1008
C	1.9825	-0.7683	-0.1123
C	1.9684	0.6805	-0.5985
C	3.3822	1.1831	-0.8988
C	4.2979	1.0199	0.3157
H	4.7680	-1.0655	0.0548
H	4.9203	-0.5162	1.7123
H	2.4482	-0.3564	1.9264
H	2.8961	-1.9747	1.4077
H	2.3819	-1.3978	-0.9236
H	1.3316	0.7649	-1.4830
H	1.5132	1.2971	0.1840
H	3.7970	0.6170	-1.7405
H	3.3501	2.2286	-1.2150
H	3.9464	1.6757	1.1201
H	5.3136	1.3407	0.0708
O	0.6861	-1.2254	0.2485
H	-1.5878	-1.6879	-2.1125
C	-3.0918	1.7415	0.3219
C	-1.9743	1.0773	-0.4854
C	-2.4287	-0.2628	-1.0401
C	-2.9152	-1.1874	0.0704
C	-4.0365	-0.5316	0.8807
C	-3.5950	0.8231	1.4370
H	-3.9256	1.9917	-0.3437
H	-2.7335	2.6852	0.7385
H	-1.1059	0.9051	0.1559
H	-1.6493	1.7190	-1.3069
H	-3.2470	-0.0927	-1.7527
H	-3.2598	-2.1341	-0.3589
H	-2.0672	-1.4166	0.7221
H	-4.9148	-0.3902	0.2409
H	-4.3454	-1.1956	1.6908
H	-2.7913	0.6675	2.1643
H	-4.4199	1.2971	1.9742
O	-1.3162	-0.8345	-1.7556
H	0.0882	-1.1096	-0.5096

Table S13. Atomic coordinates for isomer III (= EG-(1)AG-) of the cyclohexanol dimer according to B3LYP-D3(BJ)/def2TZVP DFT calculations (principal axes system).

Atom	<i>a</i> / Å	<i>b</i> / Å	<i>c</i> / Å
C	2.1093	0.0141	1.5620
C	2.8415	1.1049	0.7770
C	2.8902	0.8264	-0.7206
C	3.4181	-0.5762	-1.0189
C	2.6603	-1.6581	-0.2479
C	2.6732	-1.3740	1.2551
H	2.1851	0.2260	2.6309
H	1.0467	0.0448	1.3164
H	3.8751	1.1812	1.1293
H	2.3748	2.0777	0.9433
H	3.5348	1.5703	-1.2023
H	4.4784	-0.6027	-0.7463
H	3.3734	-0.7631	-2.0971
H	1.6255	-1.6948	-0.5980
H	3.0992	-2.6364	-0.4570
H	2.1017	-2.1384	1.7867
H	3.7036	-1.4401	1.6243
O	1.5521	0.9914	-1.2327
H	1.5534	0.8137	-2.1790
C	-2.6961	-1.5457	-0.6774
C	-1.5238	-0.6776	-0.2161
C	-1.8728	0.8104	-0.2654
C	-3.1239	1.1006	0.5509
C	-4.3041	0.2381	0.1006
C	-3.9568	-1.2516	0.1374
H	-2.8992	-1.3489	-1.7363
H	-2.4324	-2.6038	-0.6041
H	-0.6382	-0.8659	-0.8284
H	-1.2571	-0.9296	0.8157
H	-2.0777	1.0793	-1.3145
H	-3.3631	2.1632	0.4739
H	-2.8939	0.9013	1.6029
H	-5.1754	0.4404	0.7279
H	-4.5869	0.5145	-0.9215
H	-3.7907	-1.5561	1.1768
H	-4.7956	-1.8461	-0.2335
O	-0.8262	1.6256	0.2402
H	-0.0253	1.4664	-0.2846

Table S14. Atomic coordinates for isomer IV (= EG-(1)AG+) of the cyclohexanol dimer according to B3LYP-D3(BJ)/def2TZVP DFT calculations (principal axes system).

Atom	a / Å	b / Å	c / Å
C	-2.5464	-1.4770	0.8760
C	-1.7678	-0.1811	1.1106
C	-1.7228	0.6776	-0.1523
C	-3.1265	0.9748	-0.6585
C	-3.9181	-0.3126	-0.8967
C	-3.9564	-1.1890	0.3570
H	-2.0123	-2.0924	0.1429
H	-2.5912	-2.0623	1.7977
H	-2.2455	0.4055	1.9025
H	-0.7484	-0.3959	1.4420
H	-1.1939	0.1073	-0.9328
H	-3.0606	1.5685	-1.5728
H	-3.6329	1.5947	0.0886
H	-3.4549	-0.8770	-1.7139
H	-4.9329	-0.0725	-1.2230
H	-4.5267	-0.6736	1.1379
H	-4.4829	-2.1241	0.1494
O	-1.0607	1.9150	0.0651
H	1.9386	1.5825	1.7388
C	3.5015	-1.1336	0.6669
C	3.8053	0.3453	0.4198
C	2.5797	1.1129	-0.0736
C	1.9462	0.4422	-1.2868
C	1.6479	-1.0384	-1.0418
C	2.8970	-1.7886	-0.5764
H	4.4139	-1.6532	0.9682
H	2.7971	-1.2229	1.4984
H	4.1943	0.8185	1.3275
H	4.5906	0.4407	-0.3374
H	2.8674	2.1367	-0.3368
H	2.6448	0.5422	-2.1232
H	1.0402	0.9847	-1.5621
H	1.2501	-1.4878	-1.9545
H	0.8686	-1.1295	-0.2817
H	2.6560	-2.8343	-0.3715
H	3.6407	-1.7901	-1.3818
O	1.5659	1.1713	0.9514
H	-0.1748	1.7274	0.4166

Table S15. Atomic coordinates for isomer V (= AG-(1)EG+) of the cyclohexanol dimer according to B3LYP-D3(BJ)/def2TZVP DFT calculations (principal axes system).

Atom	a / Å	b / Å	c / Å
C	1.9313	-1.3224	-0.8491
C	2.0610	0.1144	-1.3569
C	2.2607	1.1128	-0.2116
C	3.4388	0.7080	0.6695
C	3.3110	-0.7296	1.1771
C	3.1284	-1.7132	0.0194
H	1.0188	-1.4117	-0.2534
H	1.8282	-2.0097	-1.6927
H	2.9200	0.1881	-2.0332
H	1.1806	0.4024	-1.9375
H	2.4625	2.1043	-0.6384
H	4.3578	0.8096	0.0829
H	3.5096	1.4069	1.5056
H	2.4491	-0.7946	1.8461
H	4.1924	-0.9954	1.7662
H	3.0031	-2.7297	0.4013
H	4.0351	-1.7197	-0.5973
O	1.1078	1.1858	0.6251
H	0.3525	1.4977	0.0985
C	-2.9136	-1.3455	-0.9319
C	-1.9439	-0.1924	-1.1979
C	-2.3018	1.0281	-0.3667
C	-2.3587	0.6944	1.1203
C	-3.3335	-0.4543	1.3912
C	-2.9783	-1.6866	0.5578
H	-2.6113	-2.2207	-1.5109
H	-3.9144	-1.0703	-1.2829
H	-1.9365	0.0783	-2.2557
H	-0.9286	-0.4990	-0.9354
H	-3.2823	1.4019	-0.6909
H	-2.6502	1.5836	1.6887
H	-1.3529	0.4179	1.4490
H	-3.3314	-0.6985	2.4556
H	-4.3529	-0.1352	1.1464
H	-3.7055	-2.4831	0.7320
H	-2.0051	-2.0708	0.8815
O	-1.3146	2.0398	-0.6454
H	-1.5451	2.8368	-0.1541

Table S16. Atomic coordinates for isomer VI (= EG-(1)EG+) of the cyclohexanol dimer according to B3LYP-D3(BJ)/def2TZVP DFT calculations (principal axes system).

Atom	a / Å	b / Å	c / Å
C	-3.8059	-1.5092	-0.0227
C	-2.6044	-1.1656	-0.9050
C	-1.7360	-0.0884	-0.2725
C	-2.5576	1.1576	0.0551
C	-3.7564	0.8220	0.9452
C	-4.6289	-0.2640	0.3134
H	-3.4534	-1.9673	0.9085
H	-4.4313	-2.2561	-0.5175
H	-2.9467	-0.7965	-1.8774
H	-1.9949	-2.0512	-1.0982
H	-1.3270	-0.4853	0.6708
H	-1.9154	1.9002	0.5367
H	-2.9021	1.5927	-0.8890
H	-3.3979	0.4728	1.9201
H	-4.3460	1.7220	1.1366
H	-5.0796	0.1273	-0.6055
H	-5.4539	-0.5241	0.9815
O	-0.6716	0.1979	-1.1690
H	1.4817	2.6356	-0.4662
C	4.1361	-0.3878	-0.8164
C	2.9600	0.5673	-1.0363
C	2.4010	1.0632	0.2926
C	1.9889	-0.0952	1.1864
C	3.1608	-1.0522	1.4155
C	3.7380	-1.5536	0.0905
H	4.9688	0.1578	-0.3585
H	4.4980	-0.7578	-1.7779
H	2.1574	0.0552	-1.5750
H	3.2714	1.4192	-1.6497
H	3.1691	1.6536	0.8100
H	1.6094	0.2944	2.1332
H	1.1674	-0.6278	0.6989
H	3.9466	-0.5388	1.9808
H	2.8346	-1.8929	2.0313
H	2.9867	-2.1650	-0.4202
H	4.5996	-2.1998	0.2740
O	1.2407	1.8951	0.1022
H	-0.0876	0.8540	-0.7518

Table S17. Results from a second-order intramonomer / third-order intermonomer Symmetry-Adapted Perturbation Theory (SAPT2+(3)/aug-cc-pVDZ) binding energy decomposition of $(\text{cyclohexanol})_2$ and related dimers, comparing the magnitude of the electrostatic and dispersion contributions, together with available reference values from the S22 database (all values in kJ mol^{-1}).

	$\Delta E_{\text{Electrostatic}}$	$\Delta E_{\text{Dispersion}}$	ΔE_{Ind}	ΔE_{Exch}	ΔE_{Total}	$\Delta E_{\text{S22}}^{[f]}$
$(\text{H}_2\text{O})_2$ ^[a]	-35.7 [191.9%]	-9.5 [50.8%]	-11.1	37.7	-18.6	-21.0
$(\text{Cyclohexanol})_2$ ^[b]	-46.5 [159.2%]	-26.6 [91.2%]	-16.6	60.5	-29.2	
$(\text{Phenol})_2$ ^[c]	-41.8 [151.3%]	-28.8 [104.3%]	-15.9	58.9	-27.6	-29.5
$(2\text{-Adamantanol})_2$ ^[b]	-44.8 [136.2%]	-35.2 [107.0%]	-16.2	63.3	-32.9	
$(\text{Cyclohexylamine})_2$ ^[b]	-30.0 [138.1%]	-31.4 [144.5%]	-9.3	48.9	-21.7	
$(\text{H}_2\text{S})_2$ ^[d]	-12.1 [223.7%]	-7.8 [144.5%]	-4.7	19.2	-5.4	
Pyridine-CH_4 ^[e]	-3.0 [57.5%]	-10.9 [208.1%]	-0.7	9.4	-5.2	

^[a]T. R. Dyke, K. M. Mack, J. S. Muenter, *J. Chem. Phys.*, **1977**, *66*, 498–510. ^[b]This work. ^[c]N. A. Seifert, A. L. Steber, J. L. Neill, C. Pérez, D. P. Zaleski, B. H. Pate, A. Lesarri, *Phys. Chem. Chem. Phys.* **2013**, *15*, 11468–11477. ^[d]A. Das, P. K. Mandal, F. J. Lovas, C. Medcraft, N. R. Walker, E. Arunan, *Angew. Chem. Int. Ed.*, **2018**, *57*, 15199–15203. ^[e]Q. Gou, L. Spada, M. Vallejo-López, A. Lesarri, E. J. Cocinero, W. Caminati, *Phys. Chem. Chem. Phys.*, **2014**, *16*, 13041–13046. ^[f] ΔE_{S22} corresponds to the interaction energies presented in Hobza's S22 database, recalculated by Sherrill: T. Takatani, E. G. Hohenstein, M. Malagoli, M. S. Marshall, C. D. Sherrill, *J. Chem. Phys.*, **2010**, *132*, 144104.